Article

Stochastic Coordinated Management of Electrical–Gas–Thermal Networks in Flexible Energy Hubs Considering Day-Ahead Energy and Ancillary Markets

Sina Parhoudeh [1],* , **Pablo Eguía López [1]** and **Abdollah Kavousi Fard [2]**

[1] Department of Electrical Engineering, Faculty of Engineering of Bilbao, University of the Basque Country (UPV/EHU), Plaza Ingeniero Torres Quevedo, 1, 48013 Bilbao, Spain; pablo.eguia@ehu.eus

[2] Department of Electrical and Electronics Engineering, Shiraz University of Technology, Shiraz 7155713876, Iran; kavousi@sutech.ac.ir

* Correspondence: sina.parhoudeh@ehu.eus

Abstract: This paper presents an optimal operation framework for electrical, gas, and thermal networks in the presence of energy hubs (EHs), so that EHs can benefit from day-ahead ancillary and energy markets. Therefore, to consider the goals of network operators (optimal operation of networks) and EHs (optimal operation in markets), the proposed model is developed in the form of a bi-level optimization. Its upper-level formulation minimizes the expected energy loss in the proposed networks based on the optimal power flow constraints and technical limits. At the lower-level problem, maximizing the expected profit of EHs in day-ahead energy and ancillary markets (including reactive and reserve regulation) is formulated based on the operational model of resources, storage devices, and responsive load in the EH framework, and the flexible constraints of EHs. This scheme includes the uncertainties of load, market price, renewable energy resources, and mobile storage energy demand, which uses the point estimation method to model them. Karush–Kuhn–Tucker is then used to extract the single-level model. Finally, by implementing the proposed scheme on a standard system, the obtained numerical results confirm the capability of the proposed model in improving the network's operation and economic status of EHs. As a result, the proposed scheme is able to decrease operation indices such as energy losses, voltage drop, and temperature drop by approximately 28.5%, 39%, and 27.8%, respectively, compared to load flow analysis. This scheme can improve the flexibility of EHs, including non-controllable sources such as renewable resources, by nearly 100% and it obtains considerable profits for hubs.

Keywords: bi-level optimization; energy and ancillary services markets; energy losses; energy networks; flexible energy hub; point estimation method

1. Introduction

1.1. Motivation

Organizations and governments encourage consumers of different energies to use clean energy and technologies with low environmental pollution and high efficiency to reduce the environmental effects of conventional energy sources and decarbonize the energy system [1]. One solution is to use combined heat and power (CHP) systems in the place of consumption [2]. Using CHP as a local source provides electric and thermal energy using gas energy as the source. In addition to increasing the efficiency of energy production, this solution will reduce the losses in the transmission system. Furthermore, these sources have much lower pollution than conventional fuel power plants [2]. In addition to CHP, renewable energy sources (RESs) and electric vehicles (EVs) are other technologies that can help reduce environmental pollution [3]. Moreover, the energy storage system (ESS) and demand response program (DRP) can also be used in the direction of the proposed goal [3]. Furthermore, they can improve network status by peak shaving [3]. This goal

will be achieved if the appropriate energy management of these elements is implemented. With this aim, it is better to consider these elements within an integrated network in the form of an energy hub (EH) [4]. For example, an industrial unit can operate as an energy hub to manage the energy of its resources and loads. Therefore, the following benefits and goals can be extracted [5]:

- Coordination between sources and active loads (ESS, EV, and DRP) in the form of energy hubs can provide technical and economic benefits for each element. For example, the presence of ESSs in an EH including renewable resources can increase the flexibility of the EH in energy networks.
- Appropriate energy management for EHs can provide the proper capabilities for the presence of hubs in energy networks such as electricity, gas, and thermal networks in terms of technical indexes (operation, reliability, flexibility, security, and economic).

In general, an energy hub is an integrated unit where sources, storage devices, and responsive loads exist alongside passive loads. Moreover, the hub is responsible for establishing coordination between the mentioned elements so that it has a central controller, and each source, storage, and load has local controllers. The local controllers are in bidirectional communication with the central controller, where each local controller sends its data, including the capacity, to the central controller. This controller then manages the energy of the mentioned elements based on its economic and technical goals and the network connected to it. Finally, it sends the command signal to the local controllers. Moreover, in the hub, several different types of energy, such as electric, thermal, and gas, can be managed. This results in increasing energy efficiency.

1.2. Literature Review

Different researchers have worked in the field of EH management in the different energy networks. The coordinated energy management of EHs in various networks based upon the hubs' cooperation in day-ahead (DA) markets has been presented in [6]. Within this method, a linear objective function towards hubs' income maximization in the DA market has been included in the problem of coordinated energy management. In this problem, the linear networks and hubs constraints have been considered. Furthermore, the uncertainties of various loads, the energy price of the DA market, the output power of RES, and the parameters of EVs have been considered in this model. Therefore, the proposed scheme has been defined as scenario-based stochastic programming (SBSP). Monte Carlo Simulation (MCS) has been considered in this programming to generate scenarios and the fast forward/backward approach was adopted to reduce the number of scenarios. The EHs' energy management has been presented in [7]. In [7], the hub is connected to the electricity, gas, and thermal networks. Moreover, EH is considered as a coordination structure between ESSs and distributed generation (DGs). The proposed problem deterministic model minimizes the energy networks' total operating expenses in the EHs' presence constrained to the equations of optimal power flow of various networks and hubs equations including storages and resources. The problem is related to the uncertainty of renewable resources, load, mobile storage, consumption energy, and energy price. Moreover, the model is a non-convex mixed-integer non-linear programming (MINLP) structure, inherently. Modeling these uncertainties has been performed by adaptive robust optimization (ARO), which is, according to an algorithm of hybrid metaheuristic, owing to the nature of the non-convexity and non-linearity of the proposed structure. A structure of multi-objective decision-making has been introduced to settle the EHs' optimum scheduling [8]. The whole EH expenses, EH average reserve, emissions, and the losses of energy have been considered by the expressed scheme simultaneously. According to the preference of EH that can be unique for each EH, these goals are prioritized. In this approach, the EH price has been introduced as the principal goal, and its cost is the highest priority. The secondary goals are included in the reserve and losses of the system and emission concurrently. A lexicography optimization has been conducted based on objective prioritization, wherein the first step includes the

minimization of the expense and the second step of the optimization is secondary goals' evaluation. The multi-energy system (MES) has been expressed in [9]. The hub manager controls the hub output electrical energy generated by combined heat and power (CHP), storage and RESs. These sources are not considered as input electrical energy and do not take part in the market. The bilateral contract and PoolCo provide input electrical energy. Furthermore, the only interfacing component of various energies is CHP. Thus, the model of this issue has been presented in the first step, including the aim of the hub energy cost minimization. The problem limitations are the limitation of indices in thermal, electrical, and gas networks and the constraints of power flow, renewable energy sources, PoolCo, storages, the models of the bilateral contract market, and CHP relations. Furthermore, the expressed information-gap decision theory (IGDT)-based robust problem model [9] has been presented in [10]. The uncertainty parameters of the proposed problem are the price of energy in the PoolCo market, loads, and the output power of RESs. Therefore, the uncertainty parameters' considered method for the expressed problem [10] is IGDT-based robust optimization. An optimization structure of flexible-reliable operation (FRO) concerning the EHs' networks of gas, electricity, and district thermal has been defined in [11]. In cooperation with CHP and RESs' structure, the incentive-based DRP (IDRP) and ESS have been considered to attain a flexible EH. The entire expected expenses of the reliability, flexibility, and operation of the power networks consisting of EHs have been minimized by the expressed scheme. The optimization program is confined to the EH structure, network reliability necessities, and the equations of the optimal power flow in the presence of IDRP and ESS (active loads, ESS). To model uncertainties of load, RESs' power production, and the accessibility of system equipment, scenario-based stochastic programming (SBSP) has been defined. The EH planning issue assessment, including ESSs, CHPs, auxiliary boilers, and wind turbines through hybrid IGDT/stochastic methods, has been presented in [12]. Furthermore, by the presented model of hybrid, the EH operator can pursue two different strategies when faced with price uncertainty, i.e., risk-seeker strategy and risk-averse strategy. This planning subject of EH has been optimized by this method in an uncertain situation by MINLP. This formulation is proposed to minimize the expected operation cost of EH where different energy demands of EH would be efficiently met. In [13], a structure of the coordinated operation of an EH according to the coupling relation linearization has been proposed, with the aim of operating energy, minimizing the operating cost, and maximizing the use of RES jointly. To consider a precise integrated EHs scheme, a combined method has been presented, which the algorithm combination including grasshopper optimization and linear weighted sum have been considered, resolving the energy management issue; therefore, the regionally coordinated optimization has been realized and the productivity of energy has improved. The EH optimum operation issue, including different energy sources, has been presented in [14] to consider the stochastic loads (thermal and electricity) inside the attendance of the expense's uncertainty and functional equations, i.e., the minimum requirements of downtime and uptime. The stochastic approach has been considered to model uncertainties of demand and cost. According to the scenario-based/data/interval gap decision technique, an optimizing structure has been presented in [15] to analyze the smart optimum EH performance subject to financial priorities, technical limitations of the distribution network, and uncertainties. The EHs with intelligent equipment and the program of demand-side management (consisting of the responsive service of load and cost) have been considered to encourage electrical buyers to choose an optimal consumption pattern. This is performed to satisfy EHs' financial priorities. Eventually, an outline of the literature has been presented in Table 1.

Table 1. Taxonomy of recent research works.

Ref.	Flexibility Model	Market Model			Uncertainty Modeling
		Energy	Reactive Power	Reserve Regulation	
[6]	No	Yes	No	No	SBSP
[7]	No	No	No	No	ARO
[8]	No	No	No	No	SBSP
[9]	No	Yes	No	No	Deterministic
[10]	No	Yes	No	No	IGDT
[11]	Yes	No	No	No	SBSP
[12]	No	No	No	No	Hybrid SBSP/IGDT
[13]	No	No	No	No	Deterministic
[14]	No	No	No	No	SBSP
[15]	No	No	No	No	Scenario-based/interval/IGDT
PM	**Yes**	**Yes**	**Yes**	**Yes**	**PEM**

1.3. Research Gaps

According to the research background and Table 1, there are the following major research gaps in the field of grid-connected EHs' energy management:

- The energy hubs can participate in the ancillary services and energy markets to make profits; however, this aspect has been less considered in most research, which has focused on how to minimize the cost of EH operation within the networks. Moreover, studies that deal with this issue have also focused on the participation of EHs in the energy market. However, there are different sources, storages, and DRPs that can control their active and reactive power. In addition, EH can store its excess power production relative to the network energy consumption; therefore, it can play a role in reserve regulation [8]. Therefore, EHs can also participate in the ancillary services market and obtain the desired financial benefit. However, this issue has rarely been discussed in other studies.

- The presence of RES in EH reduces its flexibility in the electrical sector. The dependence of the CHP thermal power on active power also reduces the flexibility of EH in the thermal sector. The low flexibility of EH leads to an unequal conclusion between DA and real-time (RT) operation. It is possible that the balance between production and supply in the energy network, including EHs, is not achieved in RT operation. Therefore, in various studies [1,5], the use of flexible sources such as storage, DRP, and renewable sources (CHP for RES, boiler for CHP) in EH has been suggested. These sources can enhance EH flexibility by RES active and CHP thermal power fluctuations' compensation in RT operation relative to DA scheduling operation. This has been stated in most studies, but fewer studies, such as [11], have concentrated on system flexibility modeling. Obtaining the values of an index needs the application of its mathematical model to the problem. By achieving the values of the index, an accurate and reliable evaluation of its pros and cons can be provided.

- In the issue of grid-connected EHs management, there are different uncertainty parameters such as load, market price, reserve demand, mobile storage energy demand, and renewable power. Therefore, it has a high number of uncertainties. In addition, the precise calculation of some indicators, such as flexibility, is required to examine different uncertainty scenarios; therefore, a reliable optimal solution can be achieved using stochastic programming. This is also not achieved by robust modeling such as ARO and IGDT, which have only the worst-case scenario. Energy management of EH is an operation problem of the power system. In this type of problem, the execution step is low and, in some cases, it reduces up to 15 min. Therefore, it is of particular importance to achieve the optimal solution in the shortest computational time. In proportion to these two cases, uncertainty modeling methods obtaining the minimum number of scenarios are required. The choice of point estimation methods

(PEM) is appropriate in this regard; however, its usage in the proposed problem has been considered in less research.

1.4. Contributions

In order to eliminate the research gap, this paper proposes the operation of energy networks in the presence of EHs in accordance with EMS. In the proposed energy management system (EMS) scheme, the local operators (resources, storages, and load operators) within EH are in bidirectional coordination with the EH operator (EHO). Local operators send their power generation and demand to EHO. Therefore, based on the energy price, reserve data, and information received from the market, EHO determines the active and reactive power optimal scheduling of the elements. EHOs are also in bidirectional coordination with energy network operators (ENOs). Accordingly, EHOs report the active and reactive power resulting from the optimal operation of EHs to the ENOs. According to the electric, gas, and thermal networks' reserve and energy demand, received information from EHs, and network operation indexes status (such as the limitation of gas/fluid flows through pipes, thermal rating of distribution lines, and voltage limitation), ENOs report the optimal operation status of EHs to EHOs. In addition, in this plan, EH has been considered a flexible system in the aforementioned networks and can benefit from DA ancillary (reactive power and reservation regulation) and energy markets simultaneously. Therefore, the proposed scheme is modeled as a two-level optimization in order to reach ENOs' goals in achieving the optimal operation status and reaching the objective of EHOs to attain desired economic and flexibility status. The upper-level problem is responsible for minimizing the expected energy losses in these networks. It also has constraints on the power dispatch equations and operation index limitations in the aforementioned networks. In the lower-level problem, maximization of expected profit of EHs in reactive power, DA ancillary, and energy markets are considered as the objective function. Constraints include the operation model of CHP, boiler, RES [16,17], DRP, mobile storage (EVs), electrical energy storage (EES) [18], thermal energy storage (TES), and the EH reserve and flexibility model. The presence of RES in EH leads to weak EH flexibility in the electrical section. However, appropriate energy management of EES, DRP, and CHP can play the role of flexible sources (FS) for elements. The CHP thermal power also depends on its active power; thus, it results in weak EH flexibility in the thermal part. However, TES, DRP, and boiler are used in this paper as FS to improve EH flexibility. Moreover, the proposed plan has uncertainties regarding the load, market price, renewable power, and EVs' energy demand. Due to the high number of uncertainty parameters, the point estimation method (PEM) is utilized for uncertainty modeling to achieve a reliable optimal solution in low computational time. PEM obtains a minimal number of scenarios compared to the other methods in stochastic programming. The Karush–Kuhn–Tucker (KKT) method is used to achieve a solvable integrated single-level problem with a conventional solver.

Finally, the innovations of this paper can be summarized as follows:

- The evaluation of flexible EH ability on energy networks' operation status.
- Simultaneous participation of flexible energy hubs in reactive power, DA reserve regulation, and energy markets to obtain high financial benefit for resources, storage devices, and aggregated responsive loads in EH format.
- Presenting a two-level problem for energy management modeling of different networks in the presence of EHs in order to simultaneously model EHOs and ENOs' objectives.
- Using PEM for many uncertainties modeling in network-connected EHs' energy management problems to achieve a reliable optimal solution in low computational time.

1.5. Paper Organization

The rest of this paper is organized as follows: Section 2 describes a two-level formulation of the proposed model based on uncertainty modeling using PEM. Section 3 extracts

a single-level integrated model based on the KKT method. Finally, numerical results and contributions are reported in Sections 4 and 5, respectively.

2. Proposed Scheme Formulation

In this section, the operation of electric, thermal, and gas energy networks in the presence of flexible EHs is presented so that EHs participate in day-ahead energy, reactive power, and reserve regulation markets. This scheme is based on a two-layer EMS. In the first layer, the operation of energy networks is optimized considering the existence of bilateral coordination between ENOs and EHO. The second layer refers to the EH energy management considering bilateral coordination between local operators (resources, storages, and load operators) and EHO. Therefore, the proposed model is formulated as a bi-level optimization so that its upper and lower levels are proportional to the first and second layers of EMS, respectively. The upper-level problem minimizes the expected energy losses of the energy networks by considering the operating constraints [19–21] of these networks. The lower-level problem is responsible for EHs' profit maximization in the mentioned markets, which includes resources operation, storage, and responsive load model, EHs' reserve formulation, and flexibility limit. Thus, the proposed problem is formulated as follows:

$$
\begin{aligned}
\min \ EEL = & \sum_{e,t,w} \pi_w \left(P_{e,t,w}^{ES} - P_{e,t,w}^{ED} + \sum_i I_{e,i}^E P_{i,t,w}^{EH} \right) \\
& + \sum_{h,t,w} \pi_w \left(H_{h,t,w}^{HS} - H_{h,t,w}^{HD} + \sum_i I_{h,i}^H H_{i,t,w}^{EH} \right) \\
& + \sum_{g,t,w} \pi_w \left(G_{g,t,w}^{GS} - G_{g,t,w}^{GD} + \sum_i I_{g,i}^G G_{i,t,w}^{EH} \right) \ .
\end{aligned}
\tag{1}
$$

Subject to:

$$
P_{e,t,w}^{ES} + \sum_i I_{e,i}^E P_{i,t,w}^{EH} - \sum_m J_{e,m}^E P_{e,m,t,w}^{EL} = P_{e,t,w}^{ED} \qquad \forall e,t,w
\tag{2}
$$

$$
Q_{e,t,w}^{ES} + \sum_i I_{e,i}^E Q_{i,t,w}^{EH} - \sum_m J_{e,m}^E Q_{e,m,t,w}^{EL} = Q_{e,t,w}^{ED} \qquad \forall e,t,w
\tag{3}
$$

$$
H_{h,t,w}^{HS} + \sum_i I_{h,i}^H H_{i,t,w}^{EH} - \sum_m J_{h,m}^H H_{h,m,t,w}^{HL} = H_{h,t,w}^{HD} \qquad \forall h,t,w
\tag{4}
$$

$$
G_{g,t,w}^{GS} + \sum_i I_{g,i}^G G_{i,t,w}^{EH} - \sum_m J_{g,m}^G G_{g,m,t,w}^{GL} = G_{g,t,w}^{GD} \qquad \forall g,t,w
\tag{5}
$$

$$
P_{e,m,t,w}^{EL} = G_{e,m}^{EL}(V_{e,t,w})^2 - V_{e,t,w}V_{m,t,w}\{G_{e,m}^{EL}\cos(\sigma_{e,t,w} - \sigma_{m,t,w}) + B_{e,m}^{EL}\sin(\sigma_{e,t,w} - \sigma_{m,t,w})\} \quad \forall e,m,t,w
\tag{6}
$$

$$
Q_{e,m,t,w}^{EL} = -B_{e,m}^{EL}(V_{e,t,w})^2 + V_{e,t,w}V_{m,t,w}\{B_{e,m}^{EL}\cos(\sigma_{e,t,w} - \sigma_{m,t,w}) - G_{e,m}^{EL}\sin(\sigma_{e,t,w} - \sigma_{m,t,w})\} \quad \forall e,m,t,w
\tag{7}
$$

$$
H_{h,m,t,w}^{HL} = \vartheta_{h,m}(T_{h,t,w} - T_{m,t,w}) \qquad \forall h,m,t,w
\tag{8}
$$

$$
G_{g,m,t,w}^{GL} = \omega_{g,m} sign(\xi_{g,t,w}, \xi_{m,t,w}) \sqrt{(\xi_{g,t,w}, \xi_{m,t,w})\left((\xi_{g,t,w})^2 - (\xi_{m,t,w})^2\right)} \quad \forall g,m,t,w
\tag{9}
$$

$$
V_{e,t,w}, T_{h,t,w}, \xi_{g,t,w} \in \left[\underline{\chi}, \overline{\chi}\right] \qquad \forall e,h,g,t,w
\tag{10}
$$

$$
\sqrt{\left(P_{e,m,t,w}^{EL}\right)^2 + \left(Q_{e,m,t,w}^{EL}\right)^2} \leq \overline{S}_{e,m}^{EL} \qquad \forall e,m,t,w
\tag{11}
$$

$$
\sqrt{\left(P_{e,t,w}^{ES}\right)^2 + \left(Q_{e,t,w}^{ES}\right)^2} \leq \overline{S}_e^{ES} \qquad \forall e = o,t,w
\tag{12}
$$

$$-\overline{G}_{g,m}^{GL}\left(\text{or }\overline{H}_{h,m}^{GL}\right) \leq G_{g,m,t,w}^{GL}\left(\text{or }H_{h,m,t,w}^{GL}\right) \leq \overline{G}_{g,m}^{GL}\left(\text{or }\overline{H}_{h,m}^{GL}\right) \qquad \forall g(\text{or }h), m, t, w \tag{13}$$

$$-\overline{G}_{g}^{GS}\left(\text{or }\overline{H}_{h}^{HS}\right) \leq G_{g,t,w}^{GS}\left(\text{or }\overline{H}_{h,t,w}^{HS}\right) \leq \overline{G}_{g}^{GS}\left(\text{or }\overline{H}_{h}^{HS}\right) \qquad \forall g(\text{or }h) = o, t, w \tag{14}$$

$$P^{EH}, Q^{EH}, G^{EH}, H^{EH} \in \arg\left\{ \max \quad \text{Profit} = \sum_{i,t,w}\left(\lambda_{t,w}^{E}\left(P_{i,t,w}^{EH} + K_Q Q_{i,t,w}^{EH}\right) + \lambda_{t,w}^{H} H_{i,t,w}^{EH} + \lambda_{t,w}^{G} G_{i,t,w}^{EH}\right) \right.$$
$$+ \sum_{i,t,w}\left(\lambda_{t,w}^{ER} ER_{i,t,w}^{EH} + \lambda_{t,w}^{HR} HR_{i,t,w}^{EH} + \lambda_{t,w}^{GR} GR_{i,t,w}^{EH}\right) . \tag{15}$$

Subject to:

$$P_{i,t,w}^{EH} + ER_{i,t,w}^{EH} = P_{i,t,w}^{C} + P_{i,t,w}^{R} + P_{i,t,w}^{D} + \left(P_{i,t,w}^{DCH} - P_{i,t,w}^{CH}\right) - P_{i,t,w}^{ED} \qquad \forall i, t, w \tag{16}$$

$$Q_{i,t,w}^{EH} = Q_{i,t,w}^{C} + Q_{i,t,w}^{R} + Q_{i,t,w}^{E} - Q_{i,t,w}^{ED} \qquad \forall i, t, w \tag{17}$$

$$H_{i,t,w}^{EH} + HR_{i,t,w}^{EH} = H_{i,t,w}^{C} + H_{i,t,w}^{B} + H_{i,t,w}^{D} + \left(H_{i,t,w}^{DCH} - H_{i,t,w}^{CH}\right) - H_{i,t,w}^{HD} \qquad \forall i, t, w \tag{18}$$

$$G_{i,t,w}^{EH} + GR_{i,t,w}^{EH} = G_{i,t,w}^{D} - G_{i,t,w}^{C} - G_{i,t,w}^{B} - G_{i,t,w}^{GD} \qquad \forall i, t, w \tag{19}$$

$$H_{i,t,w}^{C} = P_{i,t,w}^{C} \frac{(1 - \eta^{T} - \eta^{L})\eta^{H}}{\eta^{T}} \qquad \forall i, t, w \tag{20}$$

$$G_{i,t,w}^{C} = \frac{1}{\eta^{T}} P_{i,t,w}^{C} \qquad \forall i, t, w \tag{21}$$

$$\underline{P}_{i}^{C}\left(\text{or }\underline{Q}_{i}^{C}\text{ or }\underline{H}_{i}^{C}\right) \leq P_{i,t,w}^{C}\left(\text{or }Q_{i,t,w}^{C}\text{ or }H_{i,t,w}^{C}\right) \leq \overline{P}_{i}^{C}\left(\text{or }\overline{Q}_{i}^{C}\text{ or }\overline{H}_{i}^{C}\right) \qquad \forall i, t, w \tag{22}$$

$$G_{i,t,w}^{B} = \frac{1}{\eta^{B}} H_{i,t,w}^{B} \qquad \forall i, t, w \tag{23}$$

$$\underline{H}_{i}^{B} \leq H_{i,t,w}^{B} \leq \overline{H}_{i}^{B} \qquad \forall i, t, w \tag{24}$$

$$\underline{Q}_{i}^{R} \leq Q_{i,t,w}^{R} \leq \overline{Q}_{i}^{R} \qquad \forall i, t, w \tag{25}$$

$$0 \leq P_{i,t,w}^{CH}\left(\text{or }H_{i,t,w}^{CH}\right) \leq CR_{i}^{EES}\left(\text{or }CR_{i}^{TES}\right) \qquad \forall i, t, w \tag{26}$$

$$0 \leq P_{i,t,w}^{DCH}\left(\text{or }H_{i,t,w}^{DCH}\right) \leq DR_{i}^{EES}\left(\text{or }DR_{i}^{TES}\right) \qquad \forall i, t, w \tag{27}$$

$$\underline{E}_{i} \leq EI_{i} + \sum_{\tau=1}^{t}\left(\eta^{CH} P_{i,\tau,w}^{CH}\left(\text{or }H_{i,\tau,w}^{CH}\right) - \frac{1}{\eta^{DCH}} P_{i,\tau,w}^{DCH}\left(\text{or }H_{i,\tau,w}^{DCH}\right)\right) \leq \overline{E}_{i} \qquad \forall i, t, w \tag{28}$$

$$\underline{Q}_{i}^{E} \leq Q_{i,t,w}^{E} \leq \overline{Q}_{i}^{E} \qquad \forall i, t, w \tag{29}$$

$$-\beta_{i} P_{i,t,w}^{ED}\left(\text{or }H_{i,t,w}^{HD}\text{ or }G_{i,t,w}^{GD}\right) \leq P_{i,t,w}^{D}\left(\text{or }H_{i,t,w}^{D}\text{ or }G_{i,t,w}^{D}\right) \leq \beta_{i} P_{i,t,w}^{ED}\left(\text{or }H_{i,t,w}^{HD}\text{ or }G_{i,t,w}^{GD}\right) \qquad \forall i, t, w \tag{30}$$

$$\sum_{t} P_{i,t,w}^{D}\left(\text{or }H_{i,t,w}^{D}\text{ or }G_{i,t,w}^{D}\right) = 0 \qquad \forall i, w \tag{31}$$

$$ER_{i,t,w}^{EH}, HR_{i,t,w}^{EH}, GR_{i,t,w}^{EH} \geq 0 \qquad \forall i, t, w \tag{32}$$

$$\left| P_{i,t,w}^{EH} - P_{i,t,w=1}^{EH}\left(\text{or }H_{i,t,w}^{EH} - H_{i,t,w=1}^{EH}\right)\right| \leq \Delta F \qquad \forall i, t, w \right\} \tag{33}$$

(A)   Upper-level problem

This problem is presented in Equations (1)–(14). The objective function (1) is equal to minimizing the expected energy losses (*EEL*) in the electrical (first layer), thermal (second layer), and gas (third layer) networks. In this equation, the energy loss is equal to the difference between produced and consumed energy in the network and EHS. Equations (2)–(9) indicate the power distribution equations of the mentioned networks, with Equations (2)–(5) indicating active and reactive power balance in the electrical bus, the thermal power balance in the thermal node, and gas power balance in the gas node, respectively [6,7]. Active and reactive power flows in the electrical distribution lines are calculated based on Equations (6) and (7), respectively, and gas flow through the thermal (gas) pipes is determined through Equations (8) and (9) [10,11]. The aforementioned energy networks' operation limits are then modeled through Equations (10) to (14). In Equation (10), the limitation of electric buses' voltage magnitude, gas pressure, and node temperature [22,23] in each node have been stated [9]. In this regard, generally, the lower and upper limits ($\underline{\chi},\overline{\chi}$) of these variables are equal to 0.9 and 1.1, respectively [9,11]. Equations (11) and (12) express capacity limits (rated apparent power) of distribution lines and electrical distribution substations, respectively [6,7]. The limitations of the maximum gas (thermal) power flow through the pipe and gas (thermal) substation have been modeled in Equations (13) and (14), respectively [6,7]. Finally, it should be noted that the distribution substation is connected to the upstream network through slack (node) bus (*o*). Therefore, the values of the variables of P^{ES}, Q^{ES}, H^{HS}, and G^{GS} are non-zero just for the bus (node) *o*.

(B)   Lower-level problem

This problem has been modeled through Equations (15) to (33), which are used for calculating P^{EH}, Q^{EH}, H^{EH}, and G^{EH}. The objective function (15) refers to the EHs' maximization in DA reserve regulation, reactive power, and energy markets. In the first line of this equation, the EHs' financial benefit from the energy market (first, third, and fourth item) [6] and DA reactive power (second item) have been formulated. The second level of Equation (15) calculates the EHs' financial benefit obtained from the electrical (first item), thermal (second item), and gas (third item) DA reserve regulation market. In this equation, the profit in each section and hour (t) is equal to the market price and power of its section. This equation then calculates the profit (expense) of that section if the power has a positive (negative) value. According to [24], the reactive power price (K_Q) has been considered as a factor of electrical energy price (λ^E) in this equation.

The lower-level problem equations have been presented in Equations (16) to (33); thus, Equations (16)–(19) express active, reactive, thermal, and gas power balances in EH, respectively. It must be noted that, according to Equations (16), (18), and (19), the excess EH generated power (active, thermal, gas) relative to EH consumption power is delivered to the energy market or sent to the reserve regulation market. The CHP operation model has been presented in Equations (20)–(22) [2]. Equations (20) and (21) calculate the CHP thermal and gas power according to active power, respectively, and CHP output capacity is formulated using active, reactive, and thermal power in Equation (22). The CHP active and reactive power limit is known as the CHP generator capability curve. The boiler operation model has been expressed in Equations (23) and (24) [6], in which boiler input power value is calculated according to output thermal power based on (23), and its generation thermal power limit has been considered in (24). In the case of the RES models, they generally inject their maximum active power in EH proportional to weather conditions (P^R) [1]. This is because they have negligible operating costs. In this article, RES cost has been considered as zero. In addition, they are generally connected to the grid using an electronic power converter. Therefore, RESs' active and reactive power can be controlled simultaneously using the mentioned converter [25]. Therefore, in the RESs' model, it is necessary to model their reactive power limit, as achieved by Equation (25). The energy storage [26,27] operation model has been considered in Equations (26)–(29) [9,11], in which (26)–(28) are the same for EES and TES, and (29) can be used only for EES.

Equations (26) and (27) express storage devices' charge and discharge rate limits, respectively. Equations (28) and (29) model the limitation of storable energy in storage devices and controllable reactive power by EES charger, respectively. In this paper, it is assumed that the EES charger has an active front-end rectifier [25]. Thus, it is able to control EES active and reactive power simultaneously.

Alternatively, Equations (26)–(29) can be used to model electric vehicles (EVs) aggregation, except that the indexes t and w have been added to the parameters CR^{EES}, DR^{EES}, and so on [3,6]. Because it is possible that different EVs can be connected to the EH at any time and scenario, CR^{EES} at hour t is equal to the total EVs' charge rate connected to the network at this hour. The same equation holds for DR^{EES}, $\underline{E}$, $\overline{E}$, $\overline{Q}^E$, and Q^E, but EI at hour t is equal to the total new EVs' primary energy connected to the grid at this hour [3,6]. Equations (30) and (31) express the DRP operation model for electrical, thermal, and gas consumers in EH [3,11]. In this problem, DRP is based on encouragement. The consumers participating in DRP shift their energy consumption from hours with a high price (corresponding to peak hours) to hours with a low price (corresponding to off-peak hours). Therefore, in accordance with this explanation, Equation (30) refers to the power control range in the DRP scheme. Equation (31) also ensures that the total reduced energy consumption of consumers for peak hours is provided by EH in off-peak hours. The value of the reserve variable must always be positive based on Equation (32). Finally, EHs' flexibility limitation in the electrical and thermal section has been expressed by Equation (33). Low flexibility leads to the unequal result of DA operation and real-time. As a result, it is possible to have an imbalance between production and consumption in real-time operation. To compensate for this, flexible resources such as storage, DRP, and renewable resources have to compensate or eliminate the fluctuations of RESs' active power and CHPs' thermal power in each scenario compared to the corresponding scenario with the deterministic model (first scenario with the predicted value of uncertainty parameter). Under these conditions, it is expected that the difference between EHs' active (thermal) power in each scenario compared to the first scenario is low and within the flexibility tolerance (ΔF). The 100% flexibility is obtained if ΔF is equal to 0 per unit. It is noteworthy that uncertain power generation of renewable resources makes the day-ahead and real-time operation results different. Therefore, generation and consumption in real-time operation might be unbalanced. This condition is known as a low flexibility case. To compensate for this, there is a need for elements capable of power control, such as storage devices, so that they can deal with the power fluctuations of renewable resources in real-time operation compared to day-ahead operation. In this situation, flexibility is enhanced. In the thermal sector, CHP reduces flexibility as its thermal part does not have independent control from the electrical sector.

(C) Uncertainty modeling

This problem includes uncertainty parameters such as load, P^{ED}, Q^{ED}, H^{HD}, G^{GD}, market price, λ^E, λ^H, λ^G, λ^{ER}, λ^{HR}, λ^{GR}, renewable power, P^R, EVs' aggregation parameters, CR^{EES}, DR^{EES}, EI, $\underline{E}$, $\overline{Q}^E$, and Q^E. In this article, stochastic programming is used to model the uncertainties. However, due to a large number of uncertainty parameters, the point estimation method (PEM) is used to model these parameters [2]. This method extracts the least possible number of scenarios compared to the other stochastic programming methods. Hence, the confident optimal solution in low computational time is obtained. It is noteworthy that the proposed plan is a type of operation problem. Since the executive step is generally less than 1 h in operation problem, it is necessary to have a low problem-solving computational time. This article uses the PEM method based on the model of $2n + 1$, in which n and $2n + 1$ are equal to the number of uncertainty parameters and the number of extracted scenarios, respectively. The details of this method are as follows [2]:

- Step 1: definition of n.
- Step 2: define $E(S^a) = 0$ ($a = 1, 2$), a as output torque index, S as an optimization problem.

- Step 3: selection of uncertainty parameter (*Z1*).
- Step 4: calculation of skewness ($\lambda_{z_l,3}$) and kurtosis ($\lambda_{z_l,4}$) of uncertainty parameter (*Z1*) using Equations (34) and (35), respectively:

$$\lambda_{z_l,3} = \frac{E[(z_l - \mu_{z_l})^3]}{(\sigma_{z_l})^3} \tag{34}$$

$$\lambda_{z_l,4} = \frac{E[(z_l - \mu_{z_l})^4]}{(\sigma_{z_l})^4} \tag{35}$$

where μ_{z_l} and σ_{z_l} express the mean and standard deviation of variable *Z1*, respectively. $E(f)$ also expresses the mean value (expected value) of f, which is calculated for the expression inside Equations (34) and (35) as follows:

$$E[(z_l - \mu_{z_l})^3] = \sum_{j=1}^{N} (z_{l,j} - \mu_{z_l})^3 \times \text{Prob}(z_{l,j}) \tag{36}$$

$$E[(z_l - \mu_{z_l})^4] = \sum_{j=1}^{N} (z_{l,j} - \mu_{z_l})^4 \times \text{Prob}(z_{l,j}) \tag{37}$$

In the above equations, N and $\text{Prob}(z_{l,j})$ express the number of samples taken from probability distribution function *Z1* and the probability of each sample, respectively.

- Step 5: calculation of two standard locations (ξ) based on Equation (38):

$$\xi_{l,k} = \frac{\lambda_{z_l,3}}{2} + (-1)^{3-k}\sqrt{\lambda_{z_l,4} - \frac{3}{4}(\lambda_{z_l,3})^2}, \quad k = 1, 2 \tag{38}$$

- Step 6: calculation of two standard locations (ξ) based on Equation (38):

$$z_{l,k} = \mu_{z_l} + \xi_{z_l,k}.\sigma_{z_l}, \ k = 1, 2 \tag{39}$$

- Step 7: solving the confident problem in the presence of estimated locations as follows:

$$S_{l,k} = f(\mu_{z_1}, \mu_{z_2}, \dots, z_{l,k}, \dots, \mu_{z_n}) \quad k = 1, 2 \tag{40}$$

- Step 8: calculating the impact factor of (ω) using Equation (41):

$$\omega_{l,k} = (-1)^{3-k}/\xi_{l,k}(\xi_{l,1} - \xi_{l,2}), \ k = 1, 2 \tag{41}$$

- Step 9: updating first and second output torque using Equation (42):

$$E(S^a) = E(S^a) + \sum_{k=1}^{2} \omega_{l,k}.(S(l,k))^a, \quad a = 1, 2 \tag{42}$$

- Step 10: repeat steps 3 to 9, until all stochastic variables are entered in the calculations.
- Step 11: calculating the impact coefficient of the mean point using Equation (43):

$$\omega_\mu = 1 - \sum_{l=1}^{m} 1/\left(\lambda_{l,4} - (\lambda_{l,3})^2\right) \tag{43}$$

- Step 12: updating the first and second output torques using Equation (44):

$$E(S^a) = E(S^a) + \omega_\mu.(S_\mu)^a, \quad a = 1, 2 \tag{44}$$

- Step 13: calculation of mean and standard deviation of the stochastic variable using Equations (45) and (46):

$$\mu_S = E(S^1) \tag{45}$$

$$\sigma_S = \sqrt{E(S^2) - (E(S^1))^2} \tag{46}$$

The proposed scheme includes the optimization model. Optimization formulation contains an objective function [28–37]. There are different constraints in this problem [38–46]. To apply the optimization problem on the network, the grid should be equipped with intelligent devices [47–57].

3. Single-Level Modeling of the Proposed Problem

The previous presented problem, Equations (1)–(33), is a bi-level problem similar to the formulation, relations (47)–(50). Its lower-level model also has a linear programming (LP) model such as relations (48)–(50). In these relations, y expresses the variables of the lower-level problems, including EH power and reserve, and the variables of EH elements' power and energy. Relation (48) is equivalent to objective function (15), relation (49) is proportional to equal relations (16)–(21), (23), (31), and inequality relations (22), (24)–(30), and (32)–(33) appear in relation (50).

$$\text{Upper-level model, (1)–(14)} \tag{47}$$

$$y \in \arg\Big\{ \max \ \text{Profit} = A^T y \tag{48}$$

Subject to:

$$B.y = b : \rho \tag{49}$$

$$C.y \ \leq \ c : \mu\} \tag{50}$$

In this section, the KKT method is used to extract a single-level integrated model solvable by conventional algorithms [58]. The basic requirement of this method is the convexity of the lower-level problem. However, since this issue has an LP model, then the mentioned condition has also been met. To start the KKT process, the Lagrange function (L) for the lower-level problem is first computed as Equation (51). The Lagrange function is equal to the total of the main objective, relation (48), and the penalty functions method for the problem constraints. The penalty function for the constraints $a = b$, $a \leq b$ is equal to $(b - a)$ and $\mu.\max(0, a - b)$ respectively, where $\rho \in (-\infty, +\infty)$ and $\mu \geq 0$ express Lagrangian multipliers [11].

$$L = A^T y + \rho.(b - B.y) + \mu.\max(0, C.y - c) \tag{51}$$

The single-level problem then includes the upper-level problem model Equations (1)–(14) and constraints of the KKT [58].

The constraints of the KKT are obtained from the equality of the Lagrangian function derivative to the lower-level problem variables (y) and Lagrangian coefficients (ρ, μ) with zero. Thus, the problem can be written as follows:

$$
\begin{aligned}
\min \ EEL = & \sum_{e,t,w} \pi_w \left(P_{e,t,w}^{ES} - P_{e,t,w}^{ED} + \sum_i I_{e,i}^E P_{i,t,w}^{EH} \right) \\
& + \sum_{h,t,w} \pi_w \left(H_{h,t,w}^{HS} - H_{h,t,w}^{HD} + \sum_i I_{h,i}^H H_{i,t,w}^{EH} \right) \\
& + \sum_{g,t,w} \pi_w \left(G_{g,t,w}^{GS} - G_{g,t,w}^{GD} + \sum_i I_{g,i}^G G_{i,t,w}^{EH} \right).
\end{aligned}
\tag{52}
$$

Subject to:

$$\text{Constraints (2)–(14)}\cdot \tag{53}$$

$$B.\rho + C.\mu = A : \frac{\partial L}{\partial y} = 0\cdot \tag{54}$$

$$\text{Constraint (49) (or Constraints (16)–(21), (23), and (31)) :}\ \frac{\partial L}{\partial \rho} = 0 \tag{55}$$

$$\text{Constraint (50) (or Constraints (22), (24)–(30), and (32)–(34)) :}\ \frac{\partial L}{\partial \mu} = 0, \text{first condition of KKT} \tag{56}$$

$$(C.y - c).\mu = 0 : \frac{\partial L}{\partial \mu} = 0, \text{second condition of KKT} \tag{57}$$

$$\rho \in (-\infty, +\infty),\ \mu \geq 0 \tag{58}$$

The upper-level problem model has been expressed in Constraints (52) and (53), where its objective function has been considered as a single-level problem objective in (52). Its constraints (2)–(14) are also considered in Constraint (53) for the single-level problem. Relations (54)–(58) express the KKT model for the lower-level problem (15)–(33). Constraint (54) is obtained from the equality of the Lagrangian function derivative to the lower-level formulation variables with ($\frac{\partial L}{\partial y} = 0$) [58]. Constraint (55) is also obtained from $\frac{\partial L}{\partial \rho} = 0$, which includes equal relations (16)–(21), (23), and (31) in lower-level problems. It is worth mentioning that $\frac{\partial L}{\partial \mu} = 0$ has two conditions which are known as the first and second conditions of KKT [58]. In the first condition of KKT, the unequal conditions (22), (24)–(30), (32), and (33) are derived similarly to Constraint (56), from $\frac{\partial L}{\partial \mu} = 0$. In the second condition of KKT, the equality of the multiplication of the Lagrangian coefficient μ and inequality constraint boundary equation, $C.y - c$, to zero is derived from $\frac{\partial L}{\partial \mu} = 0$, which has been presented in Constraint (57) [58]. Finally, the range of Lagrange coefficients changes has been considered in Constraint (58).

4. Numerical Result and Discussion

4.1. Problem Data

The proposed scheme in this section is presented based on the multi-energy system in Figure 1, which has an IEEE 33-bus electrical distribution network [59], Madumvej 15-node thermal network [60], and a 4-node gas network [6]. The base power for electrical, thermal, and gas networks is 1 MVA, 1 MW, and 1 MW, respectively. The base voltage, temperature, and pressure are 12.66 kV, 373.15 K, and 10 bar, respectively. Slack bus in electrical, heating, and gas networks is 1, 0, and 1, respectively. The lower and upper limits of these parameters are 0.9 and 1.1 per unit. The data of the mentioned networks, including lines, substations, and load values, are reported in [6,59,60]. The active and reactive peak load of the electrical network are 3.715 MW and 2.3 MVAr, respectively, and the peak thermal load for the thermal network is equal to 3 MW [59,60]. The gas network is assumed to provide the required gas energy only for boilers and CHPs in EHs; therefore, the passive gas load value is considered as zero. Hourly load data in each network are obtained by multiplying the peak load with a load coefficient curve [61–70], where this curve has been presented in [6]. The energy price for different networks has been taken from [11], where the electricity price for the periods 1:00–7:00, 8:00–16:00 and 23:00–24:00, and 17:00–22:00 is equal to 17.6 $/MWh, 26.4 $/MWh, and 33 $/MWh, respectively. It has a value of 15 $/MWh for hours 5:00–15:00 and 22 $/MWh for other hours in the thermal network. It also has a value of 18 $/MWh for hours 5:00–22:00 and 12 $/MWh for other hours in the gas networks. The reserve price in each network is equal to the energy price in that network. Based on [24], K_Q is equal to 0.08. The system in Figure 1 has eight EHs. EH location in the different networks, peak load, and the elements in each EH are reported

in Table 2. According to this table, RES in EHs 1–6 are photovoltaic plants (PV) and wind turbines (WT). The RES peak active power is equal to 0.2 MW and 0.25MW, respectively. The active power generation daily profile of these sources is obtained by multiplying the active peak power by a daily curve of their generated power rate taken from [3]. Each of these sources is also able to control their reactive power between −0.1 MVAr and 0.1 MVAr. Regarding DRP, it is assumed that the consumers in EH participate in the DRP scheme at a rate of 40%. EHs 1–6 have two types of EES, static and mobile. The static EES is a battery (B), and the mobile type is related to the aggregation of EVs. In each of these aforementioned EHs, it is assumed that there are 80 electric vehicles. The number of connected EVs to the EH per hour is equal to the multiplication of the total number of EVs in the EH and a daily curve of their penetration rate [3]. The curve has been taken from [3], and EVs characteristics such as charge/discharge rate, charge capacity, consumption energy, and other items are reported in [3,16]. A battery with a capacity of 1.5 MWh with 90% charging and discharging efficiency has been used in the mentioned EHs. Its charge and discharge rate is equal to 0.8 MW, and the initial and minimum stored energy is 0.2 MW and 0.2 MW, respectively [6]. The battery charger can control reactive power between −0.2 MVAr and 0.2 MVAr. There are similar specifications for TES, except that its charge and discharge efficiency is 80%. In EHs 5–8, a boiler with a capacity (maximum thermal power) of 0.2 MW with an efficiency of 80% has been used. In each of these EHs, the CHP has a maximum (minimum) active, reactive, and thermal power equal to 0.5 MW, 0.2 MVAr, and 0.3 MW (0 MW, 0.2 MVAr, and 0 MW), respectively. Electricity, loss, and thermal efficiency in CHP are 40%, 8%, and 40%, respectively [2]. Finally, the standard deviation of uncertainty parameters is assumed to be equal to 10%, and the flexibility tolerance (ΔF) for achieving flexible EHs is equal to 0.05 per unit.
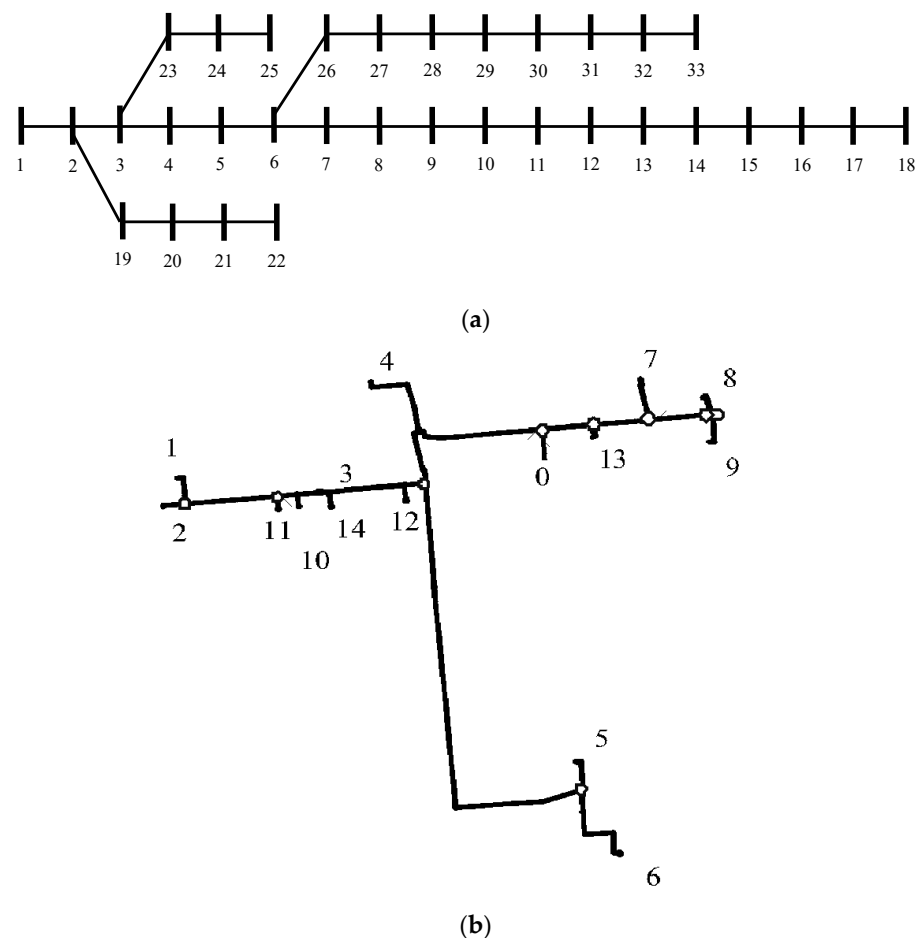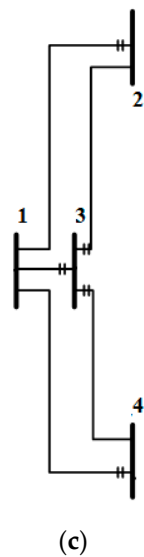

(a)

(b)

Figure 1. *Cont.*

(**c**)

Figure 1. Case test system: (**a**) IEEE 33-bus electrical distribution network [59], (**b**) 15-node Madumvej district heating grid [60], and (**c**) 4-node gas system [6].

Table 2. EHs' data.

EH	Location (e, h, g)	Source	ESS	DRP	P^{ED} (MW)	Q^{ED} (MVAr)	H^{HD} (MW)	G^{GD} (MW)
1	6, -, -	PV, WT	B, EVs	Electrical	0.6	0.3	0	0
2	13, -, -	PV, WT	B, EVs	Electrical	0.4	0.2	0	0
3	23, -, -	PV, WT	B, EVs	Electrical	0.6	0.3	0	0
4	26, -, -	PV, WT	B, EVs	Electrical	0.4	0.2	0	0
5	17, 5, 2	CHP, boiler, PV, WT	TES, B, EVs	Electrical and thermal	0.8	0.4	0.4	0
6	31, 11, 4	CHP, boiler, PV, WT	TES, B, EVs	Electrical and thermal	0.8	0.4	0.4	0
7	21, 2, 3	CHP, boiler	TES	Thermal	0.4	0.2	0.3	0
8	10, 8, 3	CHP, boiler	TES	Thermal	0.4	0.2	0.3	0

4.2. Results

The proposed model was simulated in accordance with the data reported in the previous section in the GAMS optimization software environment [71]. The numerical results obtained from different cases are reported below.

(A)   The convergence evaluation of the proposed problem-solving

In this section, the convergence result of the proposed problem using Evolutionary Algorithms (EA) such as Genetic Algorithm (GA) [72], Teaching–Learning Based Optimization (TLBO) [73], Grey Wolf Optimization (GWO) [74], Crew Search Algorithm (CSA) [75], and classical algorithms [71] such as CONOPT, IPOPT, LGO, MINOS, and OQNLP is reported. It is noteworthy that, to solve the Evolutionary Algorithm problem, the proposed model has been simulated in the MATLAB software environment. However, it is coded in accordance with the mathematical solver in GAMS software. In solving the problem with EA, problem decision variables such as P^C, Q^C, H^B, Q^R, P^{CH}, P^{DCH}, H^{CH}, H^{DCH}, P^D, H^D, G^D, and Q^E are defined by EA according to (22), (24)–(27), (29), and (30). Therefore, the value of dependent variables, including P^{EH}, Q^{EH}, H^{EH}, G^{EH}, ER^{EH}, HR^{EH}, GR^{EH}, H^C, $G^{C'}$, and G^B are calculated using (16)–(21) and (23), and the value of dependent variables P^{ES}, Q^{ES}, H^{HS}, G^{GS}, P^{EL}, Q^{EL}, H^{HL}, G^{GL}, V, T, σ, and ξ, are calculated using (2)–(9). The backward–forward load flow method for radial-network and Newton–Raphson method for ring-network is used to solve the constraints (2)–(9). The dependent variables ρ and μ are then calculated using (54) and (57). In the following, the fitness function value is evaluated. The fitness function is equal to the sum of the main objective function, (1), and the sum of the penalty function of constraints (10)–(14), H^C limitation in (22), (28), and (31)–(33). In other words, the penalty function methods [13] have been used to estimate the mentioned constraints.

The penalty function for the limitation of $a \leq b$ and constraint of $a = b$ are expressed as $\delta \cdot \max(0, a - b)$ and $\alpha \cdot (b - a)$, respectively, where $\delta \geq 0$ and $\alpha \in (-\infty, +\infty)$ represent the Lagrangian multipliers [11], the values of which are determined by the EA as a decision variable. The solution process continues to the point of convergence. In EA, it is generally assumed that the convergence point is reached after the maximum number of iterations, I_{max}. The population size and I_{max} have been considered to be equal to 80 and 4000, respectively. Other regulation parameters of these algorithms have been selected based on [22]. Finally, to evaluate statistical indexes in problem-solving, the problem is solved 30 times by each EA and classical mathematical algorithm. Therefore, the standard deviation of the final response is calculated.

The proposed problem convergence results with EAs and classical mathematic algorithms are reported in Table 3. Based on this table, it is clear that among the classical mathematical algorithms, LGO and OQNLP were not able to obtain the optimal and feasible solution for the proposed method. Among the other classical mathematical algorithms, the lowest EEL and the highest profit of EHs have been obtained by IPOPT. Thus, this algorithm has the lowest convergence iteration and computational time compared to CONOPT and MINOS; in other words, its convergence speed is high. Among EAs, CSA has been able to obtain the lowest EELs and the highest EHs profit with high convergence rates. By comparing EAs and classical mathematical algorithms, it can be seen that the final response standard deviation of the problem is non-zero by EAs, while it is zero for mathematical algorithms. It means that for each problem-solving iteration, a single optimal solution is obtained for a classical mathematical algorithm; however, this is not the case in EAs. In terms of this issue, it can be expressed that the CSA has the more desired condition compared to other EAs, thanks to the lower standard deviation of its response. Finally, it should be noted that the proposed problem, (52)–(58), is non-convex non-linear (due to power flow equations). Thus, the solvers obtain an optimal local solution, being the best solver for the algorithm that obtains the most optimal solution. Therefore, among EAs and classical mathematical algorithms, only IPOPT has such conditions. In addition to these conditions, it also has the highest convergence speed and zero response standard deviation. It is noted that the operation problem generally has a time step of less than an hour; thus, the low computational time is of particular importance. This is also the case with IPOPT due to its high convergence speed.

Table 3. Convergence results obtained by different solvers.

| Solver	EEL (MWh)	Profit ($)	Convergence Iteration	Convergence Time (min)	Standard Deviation of Final Solution (%)	Model State
GA	5.95	3578.1	2046	10.5	4.76	Feasible
TLBO	5.64	3696.8	1469	7.0	2.22	Feasible
GWO	5.78	3649.2	1722	8.4	3.65	Feasible
CSA	5.54	3752.3	1274	5.5	2.01	Feasible
CONOPT	5.50	3767.5	423	5.1	0	Feasible
IPOPT	5.35	3839.6	137	4.3	0	Feasible
LGO				-		Infeasible
MINOS	5.71	3687.4	522	7.3	0	Feasible
OQNLP				-		Infeasible

(B) Evaluation of EH performance

In Figures 2 and 3, the expected daily curve of EHs' active, reactive, thermal, and gas power and its elements have been depicted for a flexibility tolerance of 0.05 per unit. According to Figure 2a, the daily curve of RESs' generation power rate in [3], and the data in Sections 1–4, it is clear that RESs, such as PVs and WTs, inject their maximum active power into EHs. For example, based on [3], the PV generation power rate at hour 12:00 is equal to 1. Its generation active power peak is also equal to 0.2 per unit per EH. Because 6 hubs include PV, then PVs inject reactive power of 1.2 per unit into EHs at 12:00. CHPs also inject their maximum active power generation into EHs, which means 2 per unit (4 hubs including CHP × 0.5 per unit CHP active power capacity). According to Sections 1–4, the thermal energy price is higher than the gas energy price in all operation

hours, and the electricity price is higher than the gas price except for 5:00–7:00. Therefore, to achieve more profit for EHs based on (15), the maximum active power is necessary to be injected into the EHs by CHP. In addition, the batteries and electrical DRPs operate in charge or consumption mode in off-peak hours (1:00–7:00) and mid-peak hours (8:00–16:00 and 23:00–24:00). However, they operate in discharge mode and inject power into the EH in peak hours (17:00–22:00) when the electricity price is the highest. This issue increases the EHs' profit in the electrical energy market. EVs receive high energy from EHs in off-peak hours, which corresponds to low electric energy prices. In other words, EVs receive their necessary energy from EHs for travel in the next few days. They also perform charging operations from 12:00 to 16:00 until they inject their stored energy at this time into the EHs at peak hours (17:00–22:00). This performance results in EHs' profit improvement. It is noteworthy that, according to Figure 2a, in all operation hours, RESs inject active power. Therefore, it is necessary to observe the flexibility limitations in all operation hours. Hence, the electrical flexibility sources (i.e., EESs, DRPs, and CHPs) must be turned on at all simulation hours to control active power. Finally, the EHs' injected active power is calculated through relation (16), which has a time curve, as shown in Figure 2a. According to this figure, due to the charging operation of EESs and DRPs, EHs operate as electrical energy consumers in the period 1:00–7:00. However, in the other periods, they operate as an electrical energy generator in DA energy markets. The expected daily curve of EHs' reactive power and its elements are presented in Figure 2b. According to this figure, CHPs, RESs, and battery chargers inject constant reactive power to EHs during all operation hours, which, according to the data in Sections 1–4, is equal to the maximum reactive power of the mentioned elements. However, since the number of EVs at different hours are different based on their penetration rate curve in [3], then the daily curve of EVs' reactive power injection into EHs is as shown in Figure 2b. Thus, EVs inject high reactive power into EHs at 1:00–6:00 and 17:00–00:00, because a large number of EVs are connected to the EHs during these hours. However, their reactive power injection is low in other hours due to the low number of EVs in EHs. EHs' reactive power can be calculated through Equation (17), which has a curve as shown in Figure 2b. According to this figure, EHs behave as generators of reactive power during all operating hours. Therefore, high income can be achieved for them in the DA reactive power market. According to Figure 3a, CHPs and boilers always inject constant thermal power into the EHs, which is equal to the maximum thermal power, according to Sections 1–4. This performance is because the thermal energy price is higher than the gas price at all simulation hours, which causes the increase in EHs' profit in the energy market. TESs and thermal DRPs operate in the charger and energy consumption mode at periods of cheap thermal energy (1:00–4:00 and 16:00–24:00), while in the thermal peak-hour (5:00–15:00), they operate in the mode of thermal energy generation or discharge, corresponding to an expensive thermal energy price. This issue results in EHs' profit improving in the energy market based on (15). Finally, according to Figure 3a, EHs behave as thermal energy demand at 1:00–4:00 and 16:00–24:00, and they are energy producers at other times. Furthermore, boilers, TESs, and electrical DRPs are required to be turned on at all hours to maintain the EHs' flexibility in the thermal section because CHPs inject thermal power into EHs at all hours. In addition, the expected daily curve of EHs' gas power is depicted in Figure 3b. CHPs and boilers are gas energy consumers. According to Figures 2a and 3a, the daily curve of CHPs' active power and boiler thermal power are flat; therefore, the gas power daily curve of these sources is flat based on Equations (21) and (23) and Figure 3b. Finally, the daily curve of EHs' gas power is flat, so they behave as gas energy consumers.

The expected daily curve of EHs' reserve power in electrical and thermal networks is depicted in Figure 4, for $\Delta F = 0.05$ p.u. According to this figure, and in comparison with Figures 2a and 3a, it is clear that EHs can participate with part of the active power generated by sources, storage devices, and responsive loads into the reserve regulation market at hours that EHs behave as generators. However, during hours 1:00–7:00, electrical energy generators can only supply part of the load of EHs and EES. Therefore, EHs are

energy consumers and are not able to participate in the reserve regulation. This occurs in the thermal network for hours 1:00–4:00 and 16:00–24:00. It is noted that since no gas power generation has been considered in Sections 1–4, therefore, EHs cannot participate in the gas reserve regulation. Finally, the EHs' profit curve in DA energy, reactive power, and reserve regulation markets as a function of tolerance flexibility (Δ*F*) has been depicted in Figure 5. Based on this figure, it is clear that by increasing Δ*F*, the EHs' profit increases in the energy and reserve market; however, their profit in the reactive power market is constant. By increasing Δ*F*, the importance of the flexibility limitation in the proposed problem decreases. Therefore, ESSs and DRPs try to operate in discharge mode for fewer hours. For example, EVs, batteries, and electrical DRPs try to be turned off in mid-peak hours (8:00–16:00 and 23:00–00:00), which have a higher electrical energy price than off-peak hours. In other words, they only operate in the charge mode during the hours of low electricity prices. This increases the profits of EHs in the energy markets. ESSs and DRPs' energy consumption reduction in some hours also causes an increase in the reactive power generation capacity of EHs. They can then inject more reserve power into the reserve regulation market. Therefore, EHs' profit in the reserve regulation market increases with increasing Δ*F*. Finally, this type of resource performance of flexibility increases the EHs' profit in all mentioned markets by increasing Δ*F*, as shown in Figure 5d. This effect is sensible until a flexibility tolerance of 0.4 is reached. After this, there is a saturation effect and EHs' profit is constant.
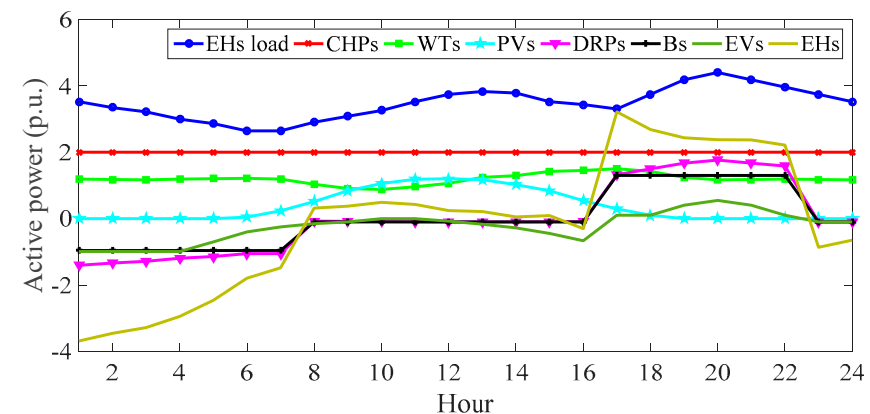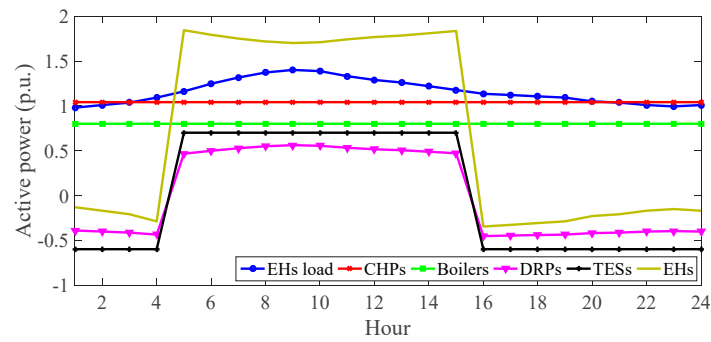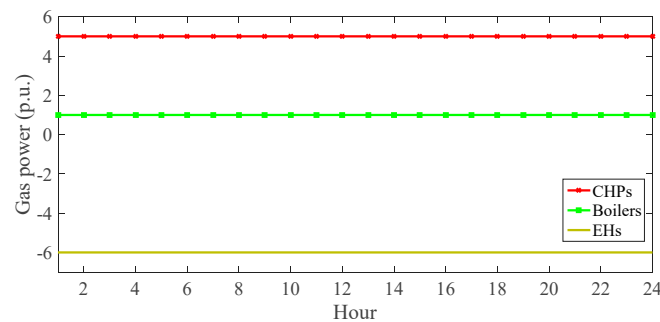

(**a**)
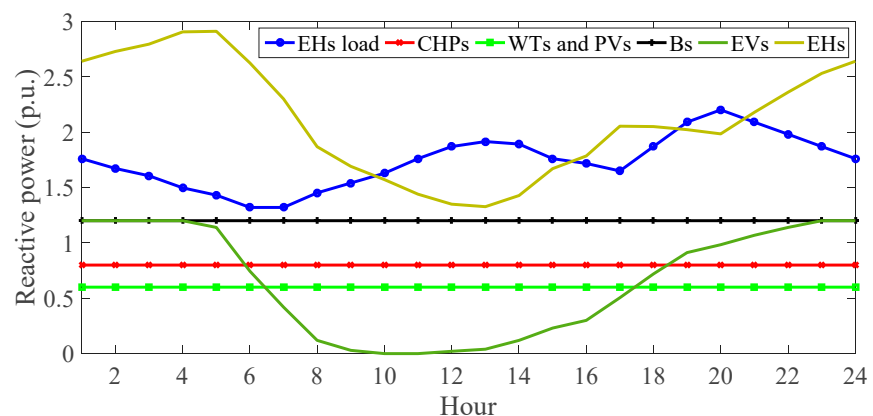
(**b**)

Figure 2. Expected daily curve of (**a**) active power and (**b**) reactive power of EHs and their elements in Δ*F* = 0.05 p.u.

(**a**)

(**b**)

Figure 3. Expected daily curve of (**a**) heating power and (**b**) gas power of EHs and their elements in $\Delta F = 0.05$ p.u.
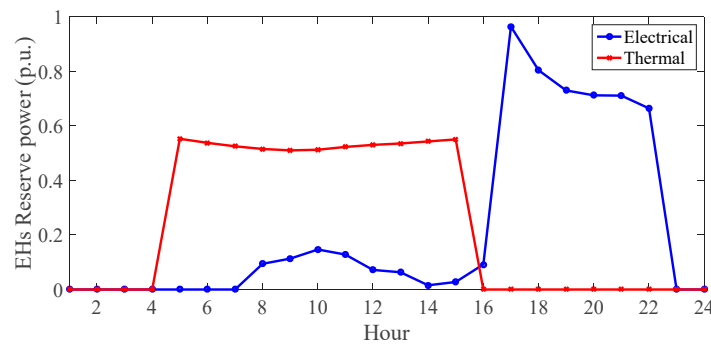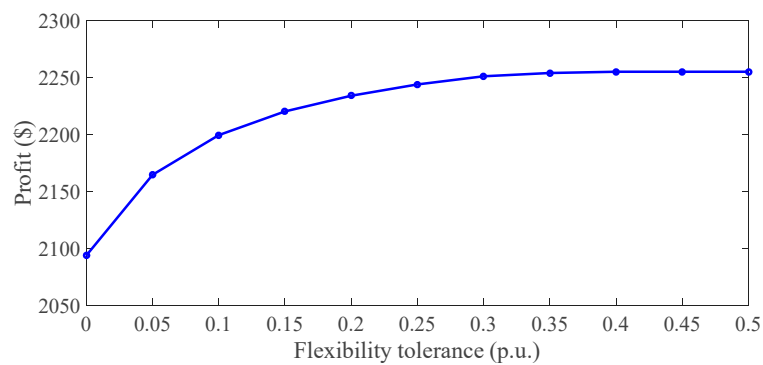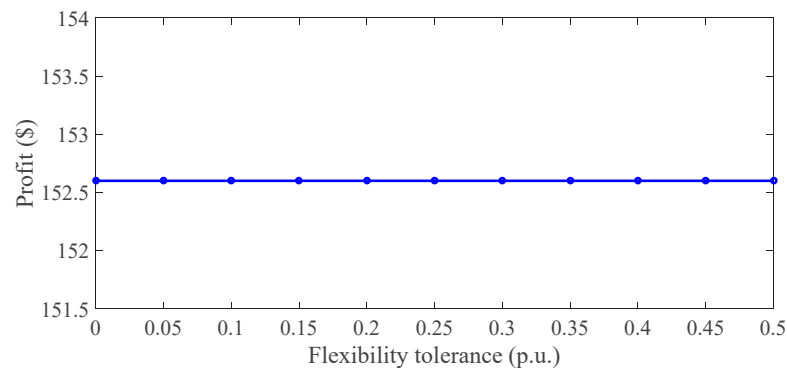

Figure 4. Expected daily EHs' reserve power curve in the electrical and district heating networks in $\Delta F = 0.05$ p.u.
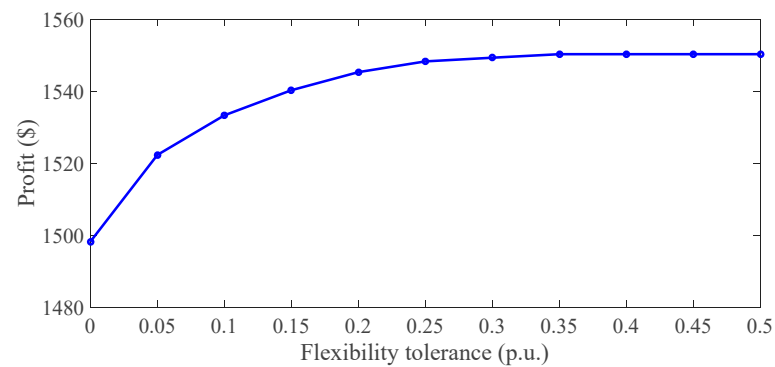

(**a**)

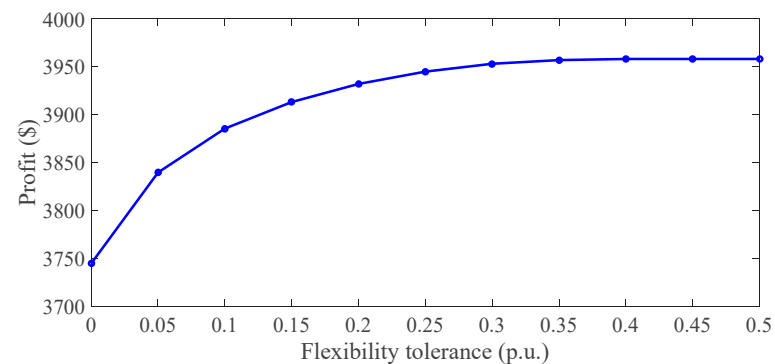**Figure 5.** *Cont*.

(b)

(c)

(d)

Figure 5. Expected curve of EHs' profit in ΔF for (**a**) DA energy market, (**b**) DA reactive power market, (**c**) DA reserve market, and (**d**) all markets.

(C) Assessing energy networks' operation status

In this section, the following case studies have been analyzed to evaluate the feasibility of the proposed model in the operation of energy networks.

Cases:

1. Power flow analysis;
2. Proposed scheme includes only EHs 1–6 that are contained only RESs;
3. Case 2 adding electrical DRP;
4. Case 3 adding EESs;
5. Case 4 adding CHP;
6. Case 5 adding thermal DRP;
7. Case 6 adding a boiler;
8. Case 7 adding TES;
9. Proposed scheme includes EHs 1–8 considering all sources, storages, and DRPs.

The results of this analysis are reported in Tables 4 and 5 for different values of flexibility tolerance (ΔF). The expected energy losses in electrical, gas, and thermal energy networks for case studies 1–9 are presented in Table 4. Due to the release problem from the limitation of the flexibility ($\Delta F = \infty$), based on Table 4, it is clear that the total EEL in mentioned networks in the load flow study (case 1) is equal to 7.48 MWh (4.42 + 3.06 + 0). However, in the presence of RES (case 2), DRPs (case 3), and EESs (case 4), the total EEL decreases. This is because in these case studies, EHs 1–6 inject active and reactive power into the consumption areas of the energy network compared to the first case. This reduces the power consumption demand of the mentioned networks from the upstream network and, consequently, reduces energy losses in the electricity network and the total EEL compared to the first case. In case 4, where RESs, electrical DRPs, and EESs have been located in EHs 1–6, the total EEL decreased to 6.13 MWh (3.07 + 3.06 + 0) compared to case 1. In case 5, by adding CHP to EHs 1–6, the losses in the electricity and thermal networks decrease, while the energy losses increase in the gas network, due to the addition of energy consumer (CHP), compared to case 4. However, the total EEL in this case study (5.84) is lower compared to case 4. With the addition of DRP in case 6, the energy losses in thermal networks decrease, compared to case 5. With the addition of a boiler in case 7, compared to case 6, the losses in thermal networks reduce, but they increase in the gas network because the boiler is a thermal energy generator and gas energy consumer. In case 8, with the addition of TES into case 7, only the energy losses in thermal networks reduce compared to case 7. Finally, considering the optimal power management of EHs 1–8, the proposed optimization scheme has been able to decrease the total EEL to 28.5%, compared to case 1. Furthermore, considering the flexibility limitation, in (33), the first, second, and fifth cases are not able to achieve a feasible solution because there is no source of flexibility in the first and second cases, and, regarding the fifth case, there is no flexible thermal source besides CHP. However, in other case studies, energy losses in electrical and thermal networks increase with decreasing ΔF. According to Figures 2a and 3a, it is clear that in the case of flexibility in EHs, ESSs and DRPs are required to operate in charge mode at hours of medium energy price, which increases losses in the mentioned networks. However, in situations where EHs' flexibility is not considered, ESSs and DRPs operate only in charge mode at hours of low energy price.

In Table 5, the maximum voltage drop (MVD), maximum temperature drop (MTD), maximum pressure drop (MPD), maximum overvoltage (MOV), maximum overpressure (MOP), and maximum overtemperature (MOT) have been reported for various case studies. According to this table, RESs, DRPs, and EESs are only effective in reducing MVD; however, CHP reduces MVD and MTD. As shown in Figure 2a,b and Figure 3a, CHP injects active, reactive, and thermal power into the electrical and thermal networks. Thus, this issue has caused overvoltage and overheating in the mentioned networks; nevertheless, according to Table 5, their value is less than the allowable value, i.e., 0.1 (1.1 − 1) per unit. CHP is also a gas consumer; therefore, in this situation, MPD increases compared to cases 1–4. In addition, thermal DRP, boilers, and TES cause MTD reduction. Besides this issue, the boiler causes an increase in MOT and MPD, but their values are lower than their maximum allowable value, i.e., 0.1 per unit. Finally, the proposed scheme for case 9, compared to the first case, was able to improve or decrease MVD and MTD by approximately 39% and 27.8%, respectively. However, these conditions are obtained by increasing MOV, MOT, and MPD by 0.04, 0.06, and 0.047 per unit, respectively. However, these values are below their maximum limits. It is noted that EHs' flexibility improvement in cases 3–4 and 6–8 corresponds to increases in MVD and MTD and decreases in MOV and MOT because in these conditions, the energy consumption hours of ESSs and DRPs increase compared to the case $\Delta F = \infty$, according to Figures 2a and 3a.

Table 4. Expected value of energy loss (MWh) in different networks for various values of ΔF.

Case	Network (ΔF = ∞)			Network (ΔF = 0.05 p.u.)			Network (ΔF = 0 p.u.)		
	Electrical	**Thermal**	**Gas**	**Electrical**	**Thermal**	**Gas**	**Electrical**	**Thermal**	**Gas**
1	4.42	3.06	0		Infeasible				
2	3.42	3.06	0		Infeasible				
3	3.28	3.06	0	3.32	3.06	0	3.37	3.06	0
4	3.07	3.06	0	3.10	3.06	0	3.14	3.06	0
5	2.52	2.54	0.78		Infeasible				
6	2.52	2.41	0.78	2.56	2.43	0.78	2.60	2.46	0.78
7	2.52	1.97	1.04	2.56	2.01	1.04	2.60	2.04	1.04
8	2.52	1.84	1.04	2.56	1.87	1.04	2.60	1.90	1.04
9	2.43	1.69	1.23	2.47	1.72	1.23	2.51	1.75	1.23

Table 5. Maximum deviation of (maximum over-) voltage, temperature, and pressure (p.u.) for various values of ΔF.

Case	(ΔF = ∞)			(ΔF = 0.05 p.u.)			(ΔF = 0 p.u.)		
	MVD/MOV	**MTD/MOT**	**MPD/MOP**	**MVD/MOV**	**MTD/MOT**	**MPD/MOP**	**MVD/MOV**	**MTD/MOT**	**MPD/MOP**
1	0.087/0	0.072/0	0/0		Infeasible				
2	0.068/0	0.072/0	0/0		Infeasible				
3	0.065/0	0.072/0	0/0	0.065/0	0.072/0	0/0	0.066/0	0.072/0	0/0
4	0.061/0	0.072/0	0/0	0.061/0	0.072/0	0/0	0.061/0	0.072/0	0/0
5	0.054/0.04	0.064/0.05	0.032/0		Infeasible				
6	0.054/0.04	0.061/0.05	0.032/0	0.054/0.04	0.061/0.05	0.032/0	0.055/0.03	0.062/0.04	0.032/0
7	0.054/0.04	0.055/0.06	0.045/0	0.054/0.04	0.055/0.06	0.045/0	0.055/0.03	0.056/0.05	0.045/0
8	0.054/0.04	0.053/0.06	0.045/0	0.054/0.04	0.053/0.06	0.045/0	0.055/0.03	0.054/0.05	0.045/0
9	0.053/0.04	0.052/0.06	0.047/0	0.053/0.04	0.052/0.06	0.047/0	0.054/0.03	0.053/0.05	0.047/0

5. Conclusions

In this paper, the operation of a flexible energy hub connected to electrical, gas, and thermal networks has been optimized. In this scheme, the energy networks pursue the minimization of energy losses, and flexible hubs seek high financial profits from energy, reactive power, and DA reserve regulation markets. Therefore, the mentioned scheme was presented in the form of a two-level optimization so that its upper level models the expected energy losses' minimization of the mentioned networks by observing the constraints of optimal power flow of these networks. In the lower-level problem, the objective function is equal to maximizing the expected profit of hubs in these markets. It is also based on the operation model of production resources, storages, responsive loads, hubs reserve formulations, and hubs' flexibility limits. To improve the optimization time, this paper proposes the use of the KKT method to extract a single-level model, and PEM models the uncertainties of load, market prices, renewable power, reservation demand, and mobile storage. Finally, by extracting numerical results from different case studies, it has been observed that classical mathematical solution algorithms have a very low responsive standard deviation compared to Evolutionary Algorithms. By high convergence speed, the IPOPT mathematical solver was also able to achieve the lowest energy losses for different networks and the highest profits for hubs. By optimal scheduling definition for active, reactive, thermal, and gas power for sources, storages, and responsive load in the form of an energy hub, the proposed scheme, compared to the load flow study, can decrease or improve the energy losses, the maximum temperature, and voltage drop by approximately 28.5%, 39%, and 27.8%, respectively. These cases have been achieved along with the increase of overvoltage and temperature and voltage drop compared to energy networks' load flow; however, their value has been lower than their allowable value. In addition, the hub flexibility improvement corresponds to an increase in energy losses, temperature, and voltage drop. Economically, the liberalizing of the problem from flexibility limitation caused an increase in the hub's profit in the energy and reservation market.

Nomenclature

1. **Acronyms**

ARO	Adaptive robust optimization
CHP	Combined heat and power
CSA	Crew Search Algorithm
DA	Day-ahead
DG	Distributed generation
DRP	Demand response program
EA	Evolutionary Algorithm
EES	Electrical energy storage
EH	Energy hub
EHO	Energy hub operator
EMS	Energy management system
ENO	Energy network operator
ESS	Energy storage system
EV	Electric vehicle
FRO	Flexible-reliable operation
FS	Flexible source
GA	Genetic Algorithm
GWO	Grey Wolf Optimization
IDRP	Incentive-based demand response program
IGDT	Information-gap decision theory
KKT	Karush–Kuhn–Tucker
LP	Linear programming
MCS	Monte Carlo Simulation
MES	Multi-energy system
MINLP	Mixed-integer non-linear programming
MOP	Maximum overpressure
MOT	Maximum overtemperature
MOV	Maximum overvoltage
MPD	Maximum pressure drop
MTD	Maximum temperature drop
MVD	Maximum voltage drop
PEM	Point estimation method
PV	Photovoltaic
RES	Renewable energy source
RT	Real-time
SBSP	Scenario-based stochastic programming
TES	Thermal energy storage
TLBO	Teaching–Learning Based Optimization
WT	Wind turbine

2. **Variables**

EEL	Expected energy losses in MWh
$ER^{EH}, HR^{EH}, GR^{EH}$	Electric, thermal, and gas reserve power (p.u.)
H^B, G^B	Boiler thermal and gas power (p.u.)
H^{CH}, H^{DCH}	Thermal power of thermal energy storage (TES) in charge and discharge mode (p.u.)
P^C, Q^C, H^C, G^C	Active, reactive, thermal, and gas power of combined heat and power (CHP) system (p.u.)
P^{CH}, P^{DCH}	Active power of electrical energy storage (EES) in charge and discharge mode (p.u.)
P^D, H^D, G^D	Active, thermal, and gas power in demand response program (DRP)
$P^{EH}, Q^{EH}, H^{EH}, G^{EH}$	Active, reactive, thermal, and gas power of energy hub (EH) (p.u.)
$P^{EL}, Q^{EL}, H^{HL}, G^{GL}$	Active and reactive power flow through electric distribution line; thermal and gas power flow through distribution pipes (p.u.)
$P^{ES}, Q^{ES}, H^{HS}, G^{GS}$	Active, reactive, thermal, and gas power passing through distribution substation (p.u.)
Profit	Total EHs' expected profits in reserve regulation, energy, and reactive markets ($)
Q^R, Q^E	Reactive power of renewable energy source (RES) and EES (p.u.)
T	Temperature (p.u.)
V, σ	Voltage magnitude (p.u.) and angle (radians)
ζ	Gas pressure (p.u.)

3. **Constants**

B^{EL}, G^{EL}	Susceptance and conductivity of electrical distribution line (p.u.)
CR^{EES}, DR^{EES}	Charge and discharge rate of EES (p.u.)
CR^{TES}, DR^{TES}	Charge and discharge rate of TES (p.u.)
$\underline{E}, \overline{E}$	Minimum and maximum storable energy in the energy storage system
(ESS) in	p.u.
EI	Initial energy of ESS (p.u.)
$\overline{G}^{GL}, \overline{G}^{GS}$	Maximum gas power flow through pipeline and gas substation (p.u.)
$\underline{H}^B, \overline{H}^B$	Minimum and maximum boiler thermal power (p.u.)
$\underline{H}^C, \overline{H}^C$	Minimum and maximum thermal power of CHP (p.u.)
$\overline{H}^{HL}, \overline{H}^{HS}$	Maximum thermal power flow through the pipeline and thermal substation (p.u.)
K_Q	Rate of reactive power price to energy price
I^E, I^H, I^G	Incidence matrix of electric bus and EH, thermal node and EH, and gas node and EH
J^E, J^H, J^G	Incidence matrix of electric bus and line, thermal node and pipeline, and gas node and pipeline
$\underline{P}^C, \overline{P}^C$	Minimum and maximum active power of CHP (p.u.)
$P^{ED}, Q^{ED}, H^{HD}, G^{GD}$	Active, reactive, thermal, and gas load (p.u.)
P^R	Generated active power of RES (p.u.)
$\underline{Q}^C, \overline{Q}^C$	Minimum and maximum reactive power of CHP (p.u.)
$\underline{Q}^E, \overline{Q}^E$	Minimum and maximum reactive power of EES (p.u.)
$\underline{Q}^R, \overline{Q}^R$	Minimum and maximum reactive power of RES (p.u.)
$\overline{S}^{EL}, \overline{S}^{ES}$	Maximum apparent power flow through the electric distribution line and substation (p.u.)
sign(a, b)	Sign function, having a value of 1 for a $\geq$ b; otherwise, it is equal to -1
β	Consumer participation rate in DRP
$\underline{\chi}, \overline{\chi}$	Minimum and maximum limits of voltage magnitude, pressure, or temperature (p.u.)
η^B	Boiler efficiency
η^{CH}, η^{DCH}	Charge and discharge efficiency of ESS

η^T, η^L, η^H	Efficiency of electricity, loss, and thermal in CHP
$\lambda^E, \lambda^H, \lambda^G$	Energy price in electric, thermal, and gas market ($/MWh)
$\lambda^{ER}, \lambda^{HR}, \lambda^{GR}$	Reserve price in the electric, thermal, and gas reserve regulation market ($/MWh)
π	Scenario occurrence probability
ω	Gas pipeline constant (p.u.)
ΔF	Flexibility tolerance (p.u.)
ϑ	Thermal pipeline constant (p.u.)

4. **Sub-indexes**

e, h, g	Electric bus, thermal node, and gas node
i	Energy hub
m	Corresponding sub-index to the bus (node)
t	Operating hours
wo	Scenario Slack (node) bus

References

1. Parhoudeh, S.; Baziar, A.; Mazareie, A.; Kavousi-Fard, A. A Novel Stochastic Framework Based on Fuzzy Cloud Theory for Modeling Uncertainty in the Micro-Grids. *Int. J. Electr. Power Energy Syst.* **2016**, *80*, 73–80. [CrossRef]
2. Homayoun, R.; Bahmani-Firouzi, B.; Niknam, T. Multi-Objective Operation of Distributed Generations and Thermal Blocks in Microgrids Based on Energy Management System. *IET Gener. Transm. Distrib.* **2021**, *15*, 1451–1462. [CrossRef]
3. Akbari, E.; Mousavi Shabestari, S.F.; Pirouzi, S.; Jadidoleslam, M. Network Flexibility Regulation by Renewable Energy Hubs Using Flexibility Pricing-Based Energy Management. Renew. *Energy* **2023**, *206*, 295–308. [CrossRef]
4. Mokaramian, E.; Shayeghi, H.; Sedaghati, F.; Safari, A.; Alhelou, H.H. A CVaR-Robust-Based Multi-Objective Optimization Model for Energy Hub Considering Uncertainty and E-Fuel Energy Storage in Energy and Reserve Markets. *IEEE Access* **2021**, *9*, 109447–109464. [CrossRef]
5. Hu, J.; Liu, X.; Shahidehpour, M.; Xia, S. Optimal Operation of Energy Hubs With Large-Scale Distributed Energy Resources for Distribution Network Congestion Management. *IEEE Trans. Sustain. Energy* **2021**, *12*, 1755–1765. [CrossRef]
6. Dini, A.; Pirouzi, S.; Norouzi, M.; Lehtonen, M. Grid-Connected Energy Hubs in the Coordinated Multi-Energy Management Based on Day-Ahead Market Framework. *Energy* **2019**, *188*, 116055. [CrossRef]
7. AkbaiZadeh, M.; Niknam, T.; Kavousi-Fard, A. Adaptive Robust Optimization for the Energy Management of the Grid-Connected Energy Hubs Based on Hybrid Meta-Heuristic Algorithm. *Energy* **2021**, *235*, 121171. [CrossRef]
8. Monemi Bidgoli, M.; Karimi, H.; Jadid, S.; Anvari-Moghaddam, A. Stochastic Electrical and Thermal Energy Management of Energy Hubs Integrated with Demand Response Programs and Renewable Energy: A Prioritized Multi-Objective Framework. *Electr. Power Syst. Res.* **2021**, *196*, 107183. [CrossRef]
9. Afrashi, K.; Bahmani-Firouzi, B.; Nafar, M. Multicarrier Energy System Management as Mixed Integer Linear Programming. *Iran. J. Sci. Technol. Trans. Electr. Eng.* **2021**, *45*, 619–631. [CrossRef]
10. Afrashi, K.; Bahmani-Firouzi, B.; Nafar, M. IGDT-Based Robust Optimization for Multicarrier Energy System Management. *Iran. J. Sci. Technol. Trans. Electr. Eng.* **2021**, *45*, 155–169. [CrossRef]
11. Dini, A.; Hassankashi, A.; Pirouzi, S.; Lehtonen, M.; Arandian, B.; Baziar, A.A. A Flexible-Reliable Operation Optimization Model of the Networked Energy Hubs with Distributed Generations, Energy Storage Systems and Demand Response. *Energy* **2022**, *239*, 121923. [CrossRef]
12. Dolatabadi, A.; Jadidbonab, M.; Mohammadi-ivatloo, B. Short-Term Scheduling Strategy for Wind-Based Energy Hub: A Hybrid Stochastic/IGDT Approach. *IEEE Trans. Sustain. Energy* **2019**, *10*, 438–448. [CrossRef]
13. Liu, J.; Wang, A.; Qu, Y.; Wang, W. Coordinated Operation of Multi-Integrated Energy System Based on Linear Weighted Sum and Grasshopper Optimization Algorithm. *IEEE Access* **2018**, *6*, 42186–42195. [CrossRef]
14. Moazeni, S.; Miragha, A.H.; Defourny, B. A Risk-Averse Stochastic Dynamic Programming Approach to Energy Hub Optimal Dispatch. *IEEE Trans. Power Syst.* **2019**, *34*, 2169–2178. [CrossRef]
15. Majidi, M.; Zare, K. Integration of Smart Energy Hubs in Distribution Networks Under Uncertainties and Demand Response Concept. *IEEE Trans. Power Syst.* **2019**, *34*, 566–574. [CrossRef]
16. Chen, J.; Sun, B.; Li, Y.; Jing, R.; Zeng, Y.; Li, M. Credible Capacity Calculation Method of Distributed Generation Based on Equal Power Supply Reliability Criterion. *Renew. Energy* **2022**, *201*, 534–547. [CrossRef]
17. Li, M.; Yang, M.; Yu, Y.; Lee, W.-J. A Wind Speed Correction Method Based on Modified Hidden Markov Model for Enhancing Wind Power Forecast. *IEEE Trans. Ind. Appl.* **2022**, *58*, 656–666. [CrossRef]
18. Zhang, X.; Wang, Y.; Yuan, X.; Shen, Y.; Lu, Z.; Wang, Z. Adaptive Dynamic Surface Control with Disturbance Observers for Battery/Supercapacitor-Based Hybrid Energy Sources in Electric Vehicles. *IEEE Trans. Transp. Electrif.* **2022**, *early access*. [CrossRef]
19. Li, P.; Hu, J.; Qiu, L.; Zhao, Y.; Ghosh, B.K. A Distributed Economic Dispatch Strategy for Power–Water Networks. *IEEE Trans. Control Netw. Syst.* **2022**, *9*, 356–366. [CrossRef]

20. Huang, N.; Zhao, X.; Guo, Y.; Cai, G.; Wang, R. Distribution Network Expansion Planning Considering a Distributed Hydrogen-Thermal Storage System Based on Photovoltaic Development of the Whole County of China. *Energy* **2023**, *278*, 127761. [CrossRef]

21. Cai, T.; Dong, M.; Chen, K.; Gong, T. Methods of Participating Power Spot Market Bidding and Settlement for Renewable Energy Systems. *Energy Rep.* **2022**, *8*, 7764–7772. [CrossRef]

22. He, Y.; Wang, F.; Du, G.; Pan, L.; Wang, K.; Gerhard, R.; Plath, R.; Rozga, P.; Trnka, P. Revisiting the Thermal Ageing on the Metallised Polypropylene Film Capacitor: From Device to Dielectric Film. *High Volt.* **2023**, *8*, 305–314. [CrossRef]

23. Huang, Z.; Li, T.; Huang, K.; Ke, H.; Lin, M.; Wang, Q. Predictions of Flow and Temperature Fields in a T-Junction Based on Dynamic Mode Decomposition and Deep Learning. *Energy* **2022**, *261*, 125228. [CrossRef]

24. Kiani, H.; Hesami, K.; Azarhooshang, A.; Pirouzi, S.; Safaee, S. Adaptive Robust Operation of the Active Distribution Network Including Renewable and Flexible Sources. *Sustain. Energy Grids Netw.* **2021**, *26*, 100476. [CrossRef]

25. Kisacikoglu, M.C.; Kesler, M.; Tolbert, L.M. Single-Phase On-Board Bidirectional PEV Charger for V2G Reactive Power Operation. *IEEE Trans. Smart Grid* **2015**, *6*, 767–775. [CrossRef]

26. Dang, W.; Liao, S.; Yang, B.; Yin, Z.; Liu, M.; Yin, L.; Zheng, W. An Encoder-Decoder Fusion Battery Life Prediction Method Based on Gaussian Process Regression and Improvement. *J. Energy Storage* **2023**, *59*, 106469. [CrossRef]

27. Min, C.; Pan, Y.; Dai, W.; Kawsar, I.; Li, Z.; Wang, G. Trajectory Optimization of an Electric Vehicle with Minimum Energy Consumption Using Inverse Dynamics Model and Servo Constraints. *Mech. Mach. Theory* **2023**, *181*, 105185. [CrossRef]

28. He, J.; Han, N.; Xia, M.; Sun, T.; Ghaebi, H. Multi-Objective Optimization and Exergoeconomic Analysis of a Multi-Generation System Based on Biogas-Steam Reforming. *Int. J. Hydrog. Energy* **2023**, *48*, 21161–21175. [CrossRef]

29. Zhang, Z.; Altalbawy, F.M.A.; Al-Bahrani, M.; Riadi, Y. Regret-Based Multi-Objective Optimization of Carbon Capture Facility in CHP-Based Microgrid with Carbon Dioxide Cycling. *J. Clean. Prod.* **2023**, *384*, 135632. [CrossRef]

30. Wang, J.; Tian, J.; Zhang, X.; Yang, B.; Liu, S.; Yin, L.; Zheng, W. Control of Time Delay Force Feedback Teleoperation System With Finite Time Convergence. *Front. Neurorobotics* **2022**, *16*, 877069. [CrossRef]

31. Yu, F.; Liu, L.; Xiao, L.; Li, K.; Cai, S. A Robust and Fixed-Time Zeroing Neural Dynamics for Computing Time-Variant Nonlinear Equation Using a Novel Nonlinear Activation Function. *Neurocomputing* **2019**, *350*, 108–116. [CrossRef]

32. Xiong, B.; Yang, K.; Zhao, J.; Li, K. Robust Dynamic Network Traffic Partitioning against Malicious Attacks. *J. Netw. Comput. Appl.* **2017**, *87*, 20–31. [CrossRef]

33. Li, W.; Ding, Y.; Yang, Y.; Sherratt, R.S.; Park, J.H.; Wang, J. Parameterized Algorithms of Fundamental NP-Hard Problems: A Survey. *Hum.-Cent. Comput. Inf. Sci.* **2020**, *10*, 29. [CrossRef]

34. Tang, Q.; Chang, L.; Yang, K.; Wang, K.; Wang, J.; Sharma, P.K. Task Number Maximization Offloading Strategy Seamlessly Adapted to UAV Scenario. *Comput. Commun.* **2020**, *151*, 19–30. [CrossRef]

35. Li, K.; Yang, W.; Li, K. Performance Analysis and Optimization for SpMV on GPU Using Probabilistic Modeling. *IEEE Trans. Parallel Distrib. Syst.* **2015**, *26*, 196–205. [CrossRef]

36. Liu, C.; Li, K.; Li, K.; Buyya, R. A New Service Mechanism for Profit Optimizations of a Cloud Provider and Its Users. *IEEE Trans. Cloud Comput.* **2021**, *9*, 14–26. [CrossRef]

37. Chen, J.; Li, K.; Li, K.; Yu, P.S.; Zeng, Z. Dynamic Planning of Bicycle Stations in Dockless Public Bicycle-Sharing System Using Gated Graph Neural Network. *ACM Trans. Intell. Syst. Technol.* **2021**, *12*, 25. [CrossRef]

38. Gu, Q.; Tian, J.; Yang, B.; Liu, M.; Gu, B.; Yin, Z.; Yin, L.; Zheng, W. A Novel Architecture of a Six Degrees of Freedom Parallel Platform. *Electronics* **2023**, *12*, 1774. [CrossRef]

39. Lin, X.; Liu, Y.; Yu, J.; Yu, R.; Zhang, J.; Wen, H. Stability Analysis of Three-Phase Grid-Connected Inverter under the Weak Grids with Asymmetrical Grid Impedance by LTP Theory in Time Domain. *Int. J. Electr. Power Energy Syst.* **2022**, *142*, 108244. [CrossRef]

40. Lin, X.; Yu, R.; Yu, J.; Wen, H. Constant-Coupling-Effect-Based PLL for Synchronization Stability Enhancement of Grid-Connected Converter Under Weak Grids. *IEEE Trans. Ind. Electron.* **2023**, *70*, 11310–11323. [CrossRef]

41. Li, K.; Tang, X.; Li, K. Energy-Efficient Stochastic Task Scheduling on Heterogeneous Computing Systems. *IEEE Trans. Parallel Distrib. Syst.* **2014**, *25*, 2867–2876. [CrossRef]

42. Li, K.; Tang, X.; Veeravalli, B.; Li, K. Scheduling Precedence Constrained Stochastic Tasks on Heterogeneous Cluster Systems. *IEEE Trans. Comput.* **2015**, *64*, 191–204. [CrossRef]

43. Wang, S.; Long, Y.; Ruby, R.; Fu, X. Clustering and Power Optimization in MmWave Massive MIMO–NOMA Systems. *Phys. Commun.* **2021**, *49*, 101469. [CrossRef]

44. Ma, Y.; Guo, Z.; Wang, L.; Zhang, J. Probabilistic Life Prediction for Reinforced Concrete Structures Subjected to Seasonal Corrosion-Fatigue Damage. *J. Struct. Eng.* **2020**, *146*, 04020117. [CrossRef]

45. Long, M.; Xiao, X. Outage Performance of Double-Relay Cooperative Transmission Network with Energy Harvesting. *Phys. Commun.* **2018**, *29*, 261–267. [CrossRef]

46. Tang, Q.; Wang, K.; Yang, K.; Luo, Y. Congestion-Balanced and Welfare-Maximized Charging Strategies for Electric Vehicles. *IEEE Trans. Parallel Distrib. Syst.* **2020**, *31*, 2882–2895. [CrossRef]

47. Wang, J.; Gao, Y.; Zhou, C.; Sherratt, R.; Wang, L. Optimal Coverage Multi-Path Scheduling Scheme with Multiple Mobile Sinks for WSNs. *Comput. Mater. Contin.* **2020**, *62*, 695–711. [CrossRef]

48. Luo, Y.; Yang, K.; Tang, Q.; Zhang, J.; Xiong, B. A Multi-Criteria Network-Aware Service Composition Algorithm in Wireless Environments. *Comput. Commun.* **2012**, *35*, 1882–1892. [CrossRef]

49. Yu, F.; Tang, Q.; Wang, W.; Wu, H. A 2.7 GHz Low-Phase-Noise LC-QVCO Using the Gate-Modulated Coupling Technique. *Wirel. Pers. Commun.* **2016**, *86*, 671–681. [CrossRef]

50. Yu, F. A Low-Voltage and Low-Power 3-GHz CMOS LC VCO for S-Band Wireless Applications. *Wirel. Pers. Commun.* **2014**, *78*, 905–914. [CrossRef]

51. Tang, Q.; Xie, M.; Yang, K.; Luo, Y.; Zhou, D.; Song, Y. A Decision Function Based Smart Charging and Discharging Strategy for Electric Vehicle in Smart Grid. *Mob. Netw. Appl.* **2019**, *24*, 1722–1731. [CrossRef]

52. Liao, Z.; Peng, J.; Huang, J.; Wang, J.; Wang, J.; Sharma, P.K.; Ghosh, U. Distributed Probabilistic Offloading in Edge Computing for 6G-Enabled Massive Internet of Things. *IEEE Internet Things J.* **2021**, *8*, 5298–5308. [CrossRef]

53. Zhang, J.; Zhong, S.; Wang, J.; Yu, X.; Alfarraj, O. A Storage Optimization Scheme for Blockchain Transaction Databases. Comput. *Syst. Sci. Eng.* **2021**, *36*, 521–535. [CrossRef]

54. Xu, Z.; Liang, W.; Li, K.-C.; Xu, J.; Jin, H. A Blockchain-Based Roadside Unit-Assisted Authentication and Key Agreement Protocol for Internet of Vehicles. *J. Parallel Distrib. Comput.* **2021**, *149*, 29–39. [CrossRef]

55. Wang, J.; Chen, W.; Wang, L.; Sherratt, R.; Alfarraj, O.; Tolba, A. Data Secure Storage Mechanism of Sensor Networks Based on Blockchain. *Comput. Mater. Contin.* **2020**, *65*, 2365–2384. [CrossRef]

56. Zhang, J.; Yang, K.; Xiang, L.; Luo, Y.; Xiong, B.; Tang, Q. A Self-Adaptive Regression-Based Multivariate Data Compression Scheme with Error Bound in Wireless Sensor Networks. *Int. J. Distrib. Sens. Netw.* **2013**, *9*, 913497. [CrossRef]

57. Tang, Q.; Yang, K.; Li, P.; Zhang, J.; Luo, Y.; Xiong, B. An Energy Efficient MCDS Construction Algorithm for Wireless Sensor Networks. *EURASIP J. Wirel. Commun. Netw.* **2012**, *2012*, 83. [CrossRef]

58. Veisi, M.; Adabi, F.; Kavousi-Fard, A.; Karimi, M. A Novel Comprehensive Energy Management Model for Multi-Microgrids Considering Ancillary Services. *IET Gener. Transm. Distrib.* **2022**, *16*, 4710–4725. [CrossRef]

59. Babu, P.R.; Rakesh, C.P.; Kumar, M.N.; Srikanth, G.; Reddy, D.P. A Novel Approach for Solving Distribution Networks. In Proceedings of the 2009 Annual IEEE India Conference, Ahmedabad, India, 19–20 December 2009; pp. 1–5.

60. Gabrielaitienė, I.; Bøhm, B.; Sundén, B. Dynamic Temperature Simulation in District Heating Systems in Denmark Regarding Pronounced Transient Behaviour. *J. Civ. Eng. Manag.* **2011**, *17*, 79–87. [CrossRef]

61. Pirouzi, S.; Zaghian, M.; Aghaei, J.; Chabok, H.; Abbasi, M.; Norouzi, M.; Shafie-khah, M.; Catalão, J.P.S. Hybrid Planning of Distributed Generation and Distribution Automation to Improve Reliability and Operation Indices. *Int. J. Electr. Power Energy Syst.* **2022**, *135*, 107540. [CrossRef]

62. Norouzi, M.; Aghaei, J.; Pirouzi, S.; Niknam, T.; Fotuhi-Firuzabad, M.; Shafie-khah, M. Hybrid Stochastic/Robust Flexible and Reliable Scheduling of Secure Networked Microgrids with Electric Springs and Electric Vehicles. *Appl. Energy* **2021**, *300*, 117395. [CrossRef]

63. Pirouzi, A.; Aghaei, J.; Pirouzi, S.; Vahidinasab, V.; Jordehi, A.R. Exploring Potential Storage-Based Flexibility Gains of Electric Vehicles in Smart Distribution Grids. *J. Energy Storage* **2022**, *52*, 105056. [CrossRef]

64. Jokar, M.R.; Shahmoradi, S.; Mohammed, A.H.; Foong, L.K.; Le, B.N.; Pirouzi, S. Stationary and Mobile Storages-Based Renewable off-Grid System Planning Considering Storage Degradation Cost Based on Information-Gap Decision Theory Optimization. *J. Energy Storage* **2023**, *58*, 106389. [CrossRef]

65. Hamidpour, H.; Aghaei, J.; Pirouzi, S.; Niknam, T.; Nikoobakht, A.; Lehtonen, M.; Shafie-khah, M.; Catalão, J.P.S. Coordinated Expansion Planning Problem Considering Wind Farms, Energy Storage Systems and Demand Response. *Energy* **2022**, *239*, 122321. [CrossRef]

66. Piltan, G.; Pirouzi, S.; Azarhooshang, A.; Rezaee Jordehi, A.; Paeizi, A.; Ghadamyari, M. Storage-Integrated Virtual Power Plants for Resiliency Enhancement of Smart Distribution Systems. *J. Energy Storage* **2022**, *55*, 105563. [CrossRef]

67. Shahbazi, A.; Aghaei, J.; Pirouzi, S.; Niknam, T.; Vahidinasab, V.; Shafie-khah, M.; Catalão, J.P.S. Holistic Approach to Resilient Electrical Energy Distribution Network Planning. *Int. J. Electr. Power Energy Syst.* **2021**, *132*, 107212. [CrossRef]

68. Parhoudeh, S.; Baziar, A.; Lopez, P.E.; Moazzen, F. Optimal Stochastic Energy Management of Smart City Incorporating Transportation System and Power Grid. *IEEE Trans. Ind. Appl.* **2020**, *early access*. [CrossRef]

69. Yan, Z.; Gao, Z.; Navesi, R.B.; Jadidoleslam, M.; Pirouzi, A. Smart Distribution Network Operation Based on Energy Management System Considering Economic-Technical Goals of Network Operator. *Energy Rep.* **2023**, *9*, 4466–4477. [CrossRef]

70. Moayed, S.H.; Shahi, H.H.; Akbarizadeh, M.; Jadidoleslam, M.; Aghatehrani, A.; Pirouzi, A. Presenting a Stochastic Model of Simultaneous Planning Problem of Distribution and Subtransmission Network Development Considering the Reliability and Security Indicators. *Int. Trans. Electr. Energy Syst.* **2023**, *2023*, e8198865. [CrossRef]

71. GAMS—General Algebraic Modeling System. Available online: https://www.gams.com/ (accessed on 1 November 2022).

72. Katoch, S.; Chauhan, S.S.; Kumar, V. A Review on Genetic Algorithm: Past, Present, and Future. *Multimed. Tools Appl.* **2021**, *80*, 8091–8126. [CrossRef]

73. Singh Gill, H.; Singh Khehra, B.; Singh, A.; Kaur, L. Teaching-Learning-Based Optimization Algorithm to Minimize Cross Entropy for Selecting Multilevel Threshold Values. *Egypt. Inform. J.* **2019**, *20*, 11–25. [CrossRef]

74. Mirjalili, S.; Mirjalili, S.; Lewis, A. Grey Wolf Optimizer. *Adv. Eng. Softw.* **2014**, *69*, 46–61. [CrossRef]

75. Askarzadeh, A. A Novel Metaheuristic Method for Solving Constrained Engineering Optimization Problems: Crow Search Algorithm. *Comput. Struct.* **2016**, *169*, 1–12. [CrossRef]